Joint Centre for Mesoscale Meteorology, Reading, UK

Tests of New Dynamics Model on the FASTEX IOP16 case

H. Lean

Internal Report No. 119
NWP Technical Paper No. 320

September 2000

Met Office Joint Centre for Mesoscale Meteorology Department of Meteorology
University of Reading PO Box 243 Reading RG6 6BB United Kingdom
Tel: +44 (0)118 931 8425 Fax: +44 (0)118 931 8791
www.metoffice.com

Designed and produced by the Met Office © Crown copyright 2001 01/0240 The Met Office logo is a registered trademark.

Tests of New Dynamics Model on the FASTEX IOP16 case

Humphrey Lean, JCMM.

September 2000

1. Introduction and Aims

The aim of the Mesoscale Modelling group at JCMM is to investigate high resolution (~1km) models for operational use. An important first step towards this is to assess the performance of the new non-hydrostatic, semi implicit, semi lagrangian model (the so called "New Dynamics" model (Staniforth et al (2000)) which will form the basis of any operational high resolution system. The purpose of this report is to describe the outcome of the first series of test runs of the New Dynamics model on the FASTEX IOP16 case.

2. Introduction to the Case

FASTEX Intensive Observation Period (IOP) 16 was a case of a rapidly moving, rapidly deepening secondary cyclone (Clough et al 1998). The period of rapid development took place between 0Z and 12Z on the 17th February 1997. The development of the surface system is shown in figure 3.1 (a) and (b). The main point of scientific interest in the case is the presence of multiple slantwise cross frontal circulations which are observed which correspond to multiple cloud heads visible in the satellite imagery (Forbes et al 2000b).

There were three reasons for working on this case. Firstly a model of a rapidly developing system is likely to be sensitive to small perturbations in both the initial state and the model properties – it would therefore be hoped that it would be easy to see the effect of making changes. Secondly being a FASTEX case there are many extra observations of the system so it would be hoped that verification of the model would be easier than in other cases. In particular in this report data from the UK C-130 aircraft (which scanned the system between 6Z and 12Z and dropped sondes) will be discussed. Data from the NOAA P3 aircraft which followed a similar pattern to the C-130 making Doppler radar measurements will also be considered. Thirdly before the start of the work reported here there was already a good deal of experience of modelling this case with the UM. This work is reported by Forbes et al (2000b) to which the reader is referred for the background information on the UM handling of the case. In general the UM handled the case well – Figure 3.1 shows the fields from the closest simulation to the observations which was a 12km, 45 level run from an analysis at the same resolution at 0Z on the 17th. These model runs reproduced similar features to much of the mesoscale structure in the system, in particular the multiple slantwise cross frontal circulations.

3. First Runs – from 50km Analysis – initial comparisons to standard UM

3.1 12km, 38 level runs and Comparison to UM

The first 12km runs carried out with the New Dynamics run were initialised from the 18Z 16th operational Limited Area Model (LAM) analysis. The LAM was a 50km, 19 level model, operational at the time of FASTEX, which covered the whole N Atlantic and much of the surrounding land. It was known from the UM work

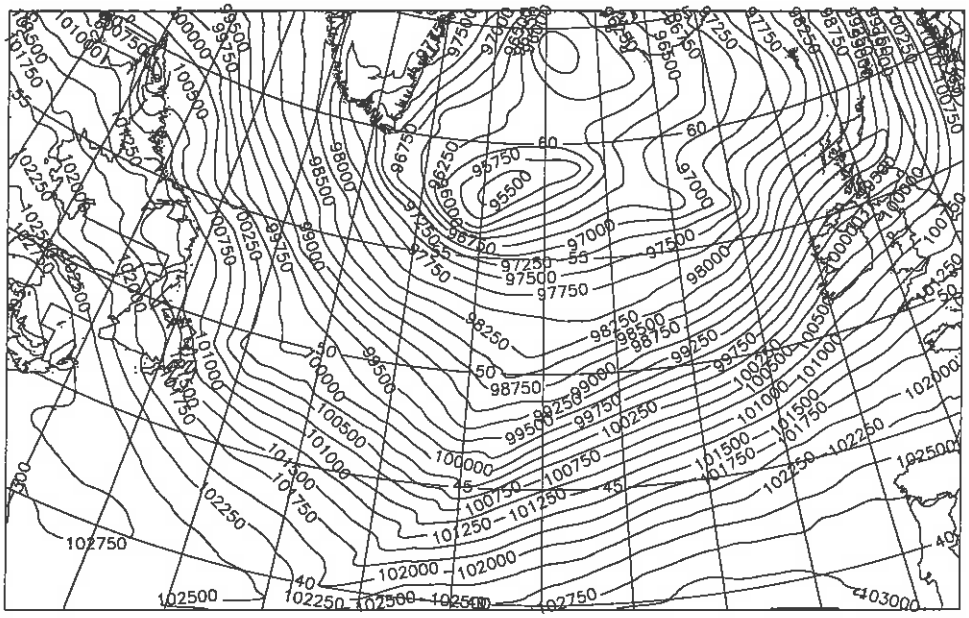

Figure 3.1(a) pmsl at 0Z 17th Feb from UM 12km analysis

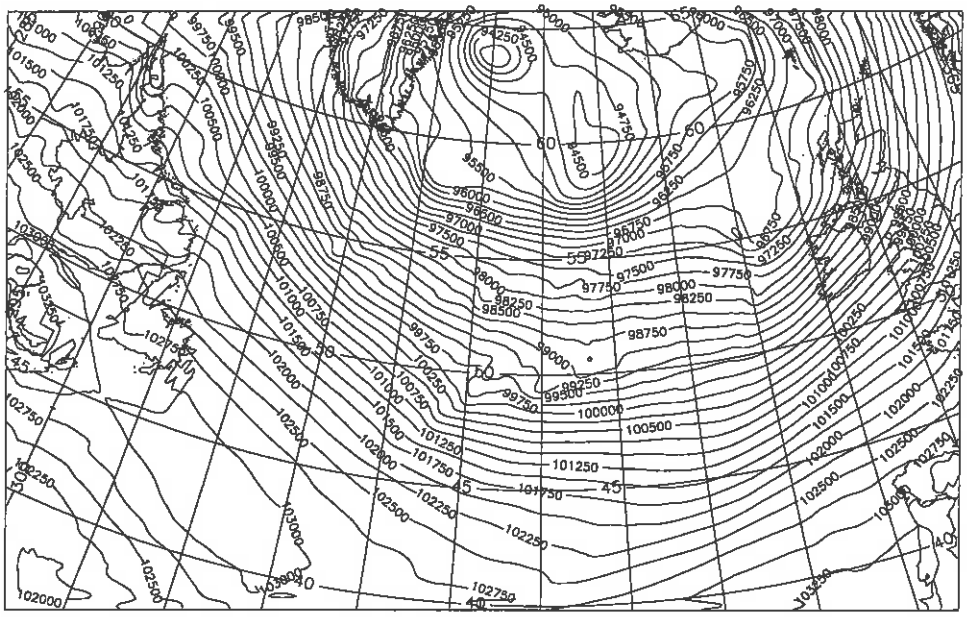

Figure 3.1(b) pmsl at 12Z Feb. T+12 forecast from UM 12km run

(Forbes et al 2000b) that forecasts run from this analysis would produce reasonable, although not the best, forecasts of the system. The forecasts were started from these 50km dumps in order to compare how the New Dynamics and UM spin up mesoscale detail from low resolution.The boundary conditions for the New Dynamics run were obtained from a global New Dynamics run from the same starting analysis (transplanted into a global dump to ensure consistency). This differs somewhat from the UM equivalent run which used boundary conditions extracted from the operational LAM model which is not possible with the current New Dynamics model. From the previous UM work the boundaries are expected to have a small effect on this model since it is being run on a relatively large domain. Throughout this section (except where otherwise stated) the UM run used for comparison to the New Dynamics was run with as close as possible to the same physics as in the New Dynamics model. These first New Dynamics runs used version 2.7 of the code and the standard 38 vertical levels approximating to those used in the UM mesoscale model.

Figure 3.2 shows a comparison between the system 1000hPa geopotential height at 12Z (i.e. a T+18 forecast) for the New Dynamics and UM.

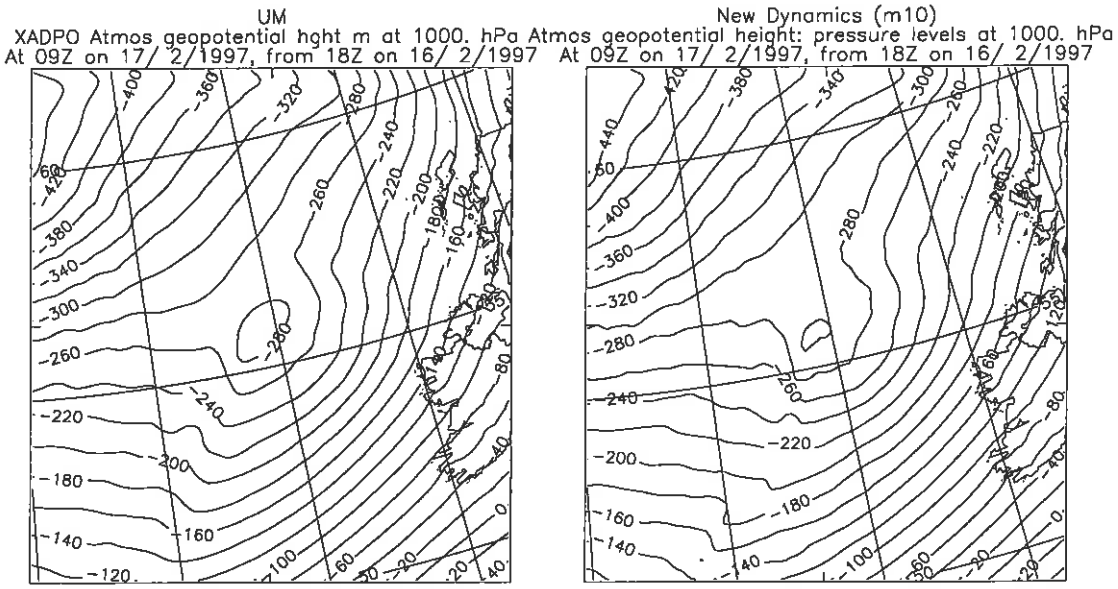

Figure 3.2 1000hPa geopotential height for UM and New Dynamics models.

The surface pressure is very similar between the two runs. There are small differences evident in the shape of the surface system (in particular in the sharpness of the trough extending to the South West from the system) and the fact that the pressure field appears somewhat more noisy in the New Dynamics. In addition the absolute values of the pressure are slightly different due to the parent low being a different depth.

However, given the fact that this is a rapidly developing system the differences may be considered to be small.

Other fields show much larger differences between the UM and the New Dynamics model. Figure 3.3 shows the 800hPa vertical velocity at 06Z (i.e. at T+12 forecast). The New Dynamics model has much sharper features – in particular the frontal features are much narrower and more coherent in the New Dynamics model. Of particular note is the third front just to the south of the northern of the two main fronts which is clearly evident in the New Dynamics run but only hinted at in the UM. Plotting similar figures with one pixel per model gridpoint shows that the fronts are about 6-8 gridpoints wide in the UM whereas they are about 1-2 gridpoints wide in the New Dynamics. The New Dynamics model behaves as if it has higher horizontal resolution which may be partly because the C grid has higher effective resolution than the B grid. It may also be expected that the higher apparent resolution is partly related to the amount of horizontal diffusion in the models. This question is addressed in the next section.

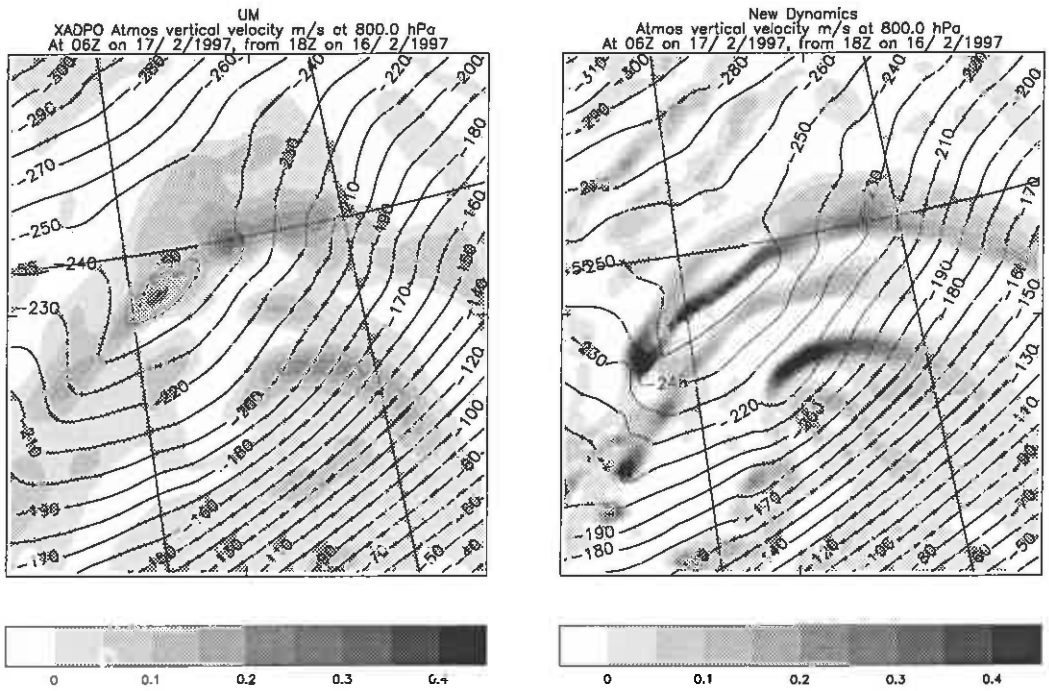

Figure 3.3 800hPa vertical velocity (shading) and 1000hPa geopotential height (contours) for UM and New Dynamics models at 06Z 17th.

3.2 Role of Horizontal Diffusion in Difference between UM and New Dynamics

In order to investigate the effect of horizontal diffusion in the UM and the New Dynamics two types of experiment were attempted. Firstly the UM was run with reduced diffusion to see if it was possible to reproduce the New Dynamics results and

secondly the opposite was attempted i.e. increasing the diffusion in the New Dynamics to the level in the UM.

The configuration in which the UM was being run was close to the operational one with changes to make the physics comparable to that in the New Dynamics. In addition the timestep was halved to avoid spurious noise emanating from the boundaries (see Forbes et al 2000b). The horizontal diffusion coefficients had been correspondingly increased by a factor of 1.4 to give the same level of damping in terms of timesteps. The diffusion in this model was therefore del-4 with a damping e-folding time for checkerboard modes of between 2.5 to 3 minutes. By contrast the New Dynamics has been run without any explicit horizontal diffusion except on the top two levels where it was retained to improve model stability. Figure 3.2 shows the effect of reducing the diffusion in the UM to 1/16 of its usual value.

The UM with 1/16 diffusion has much sharper features with variablity on spatial scales similar to those in the New Dynamics. However there are signs that the run is starting to become noisy for example northernmost frontal feature which is relatively continuous in the New Dynamics is breaking up into many separate pieces. One of the most encouraging aspects of the New Dynamics runs is that there are not just features on short spatial scales but these features are coherent (for example the fronts) rather than appearing to be noise (although as will be shown in later sections the fronts *do* break up when the New Dynamics is run at higher resolutions). The noise in the reduced diffusion UM experiment becomes even more evident at later times in the forecast (not illustrated). This experiment therefore suggests that although it is possible in this case to run the UM with reduced diffusion so as to sharpen up features the results are not comparable to those in the New Dynamics because of the tendency for features to break up into noise. It should be mentioned that experience shows that, in general, it is not possible to run the UM model with $1/16^{th}$ diffusion – in some cases the model would fail due to the growth of gridscale modes.

The second experiment mentioned above, i.e. increasing the diffusion in the New Dynamics to the UM value was also attempted. The e-folding time for damping of checkerboard modes used in the UM (2.5mins) is less than the timestep used for the New Dynamics. With diffusion coefficients calculated to give this e-folding time with del-4 diffusion on all levels the model fails after about 30 minutes model time despite the fact that the diffusion is then approximately a factor of 4 below the stability criterion. If the diffusion on the top two levels is changed to the value normally used, del-2 with an e-folding time of about 1 hour (i.e. very small) the run survives for about 6 hours but the vertical velocity field then shows a large amount of spurious noise. It is concluded that this experiment is not feasible. However it is possible to run the New Dynamics model with smaller amounts of diffusion without problems although then the diffusion is then too small to markedly affect the results.

3.3 Unmeteorological Oscillation problem

The purpose of this section is to report a problem which was encountered on the first attempt to run the New Dynamics model on this case. The problem is illustrated in figure 3.5.

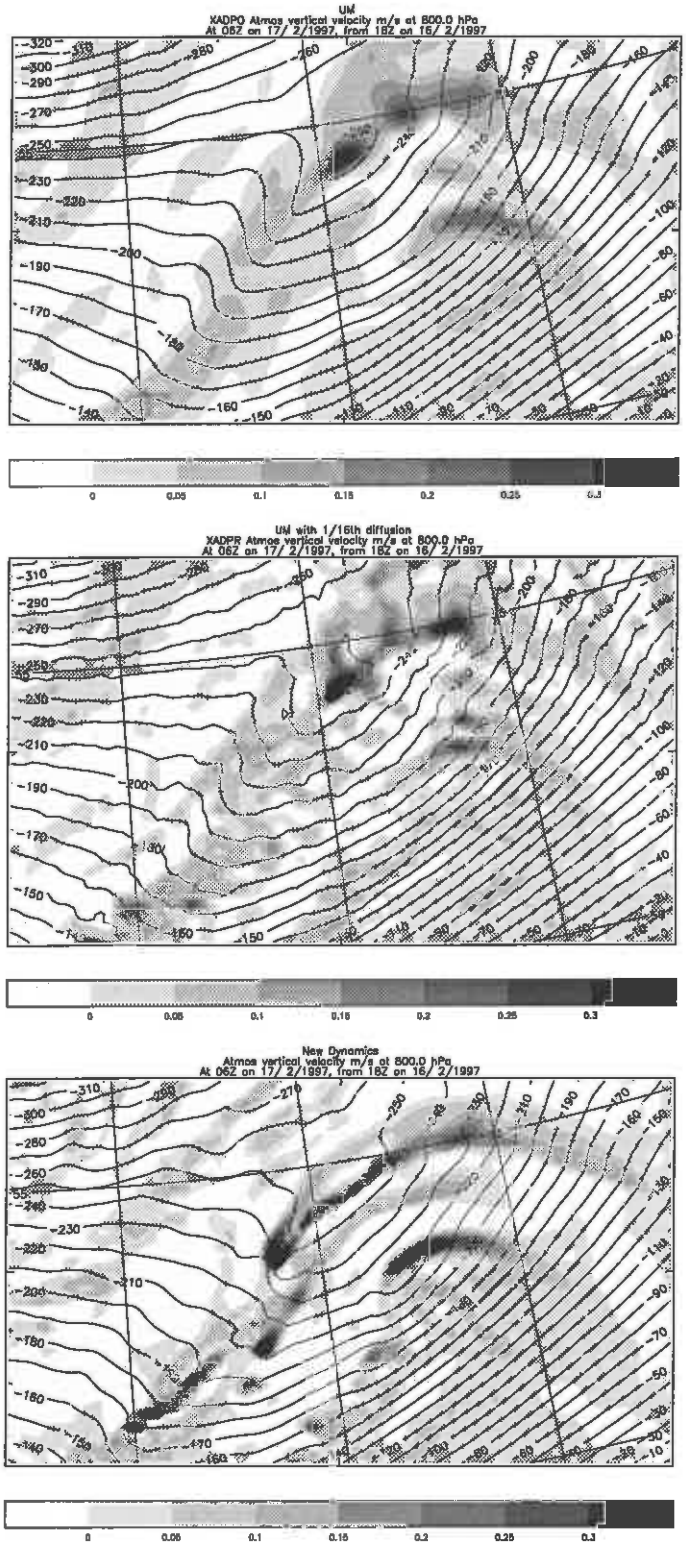

Figure 3.4 800hPa vertical velocity for UM, UM with 1/16 diffusion and New Dynamics at 6Z (T+12 forecast)

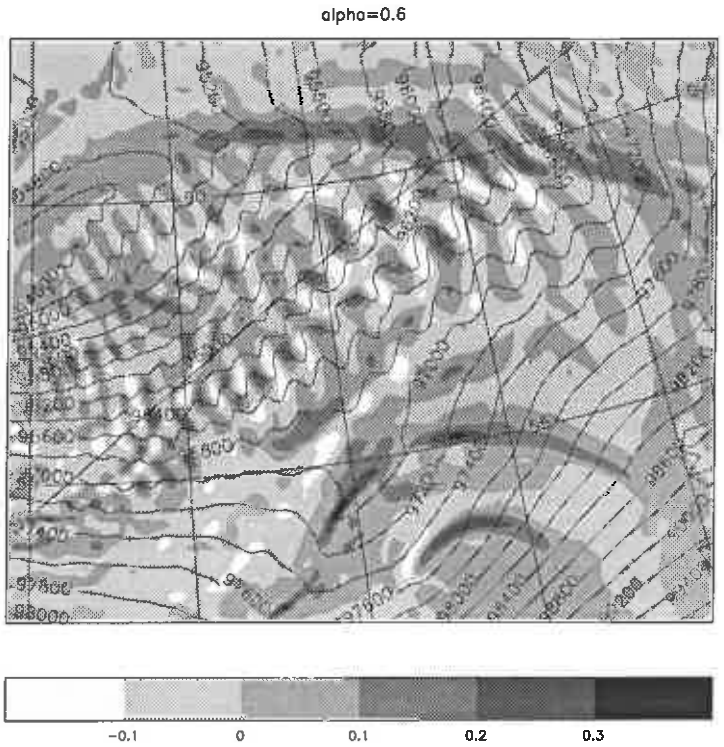

Figure 3.5 800hPa vertical velocity (shading) and 1000hPa geopotential height (contours) for 6Z (T+12 forecast).

The problem is observed in the region to the north of the system and manifests itself as waves in the 1000mb height field and a periodic structure in the vertical velocity field. After Macdonald (1999) we term this problem an oscillation rather than an instability since it becomes steady and does not continue to grow until it causes the model to fail (he refers to it as an "unmeteorological oscillation"). A cross section, Figure 3.6, shows that the oscillations appear to be greatest at upper levels in the model with maxima around 400, 250 and 50hPa. Study of the fields shows that the oscillations appear to be emanating from the shear region to the north of the jet.

The oscillation was found to be removed by either reducing the time step from 5 minutes to 3 or increasing the alpha time weighting parameters from 0.6 to 0.7. The latter was more effective and preferable being computationally cheaper. Figure 3.5 shows a comparision of cross sections, increasing alpha removes all of the oscillation leaving only a genuine feature (the front towards the right hand end of the sections) visible.

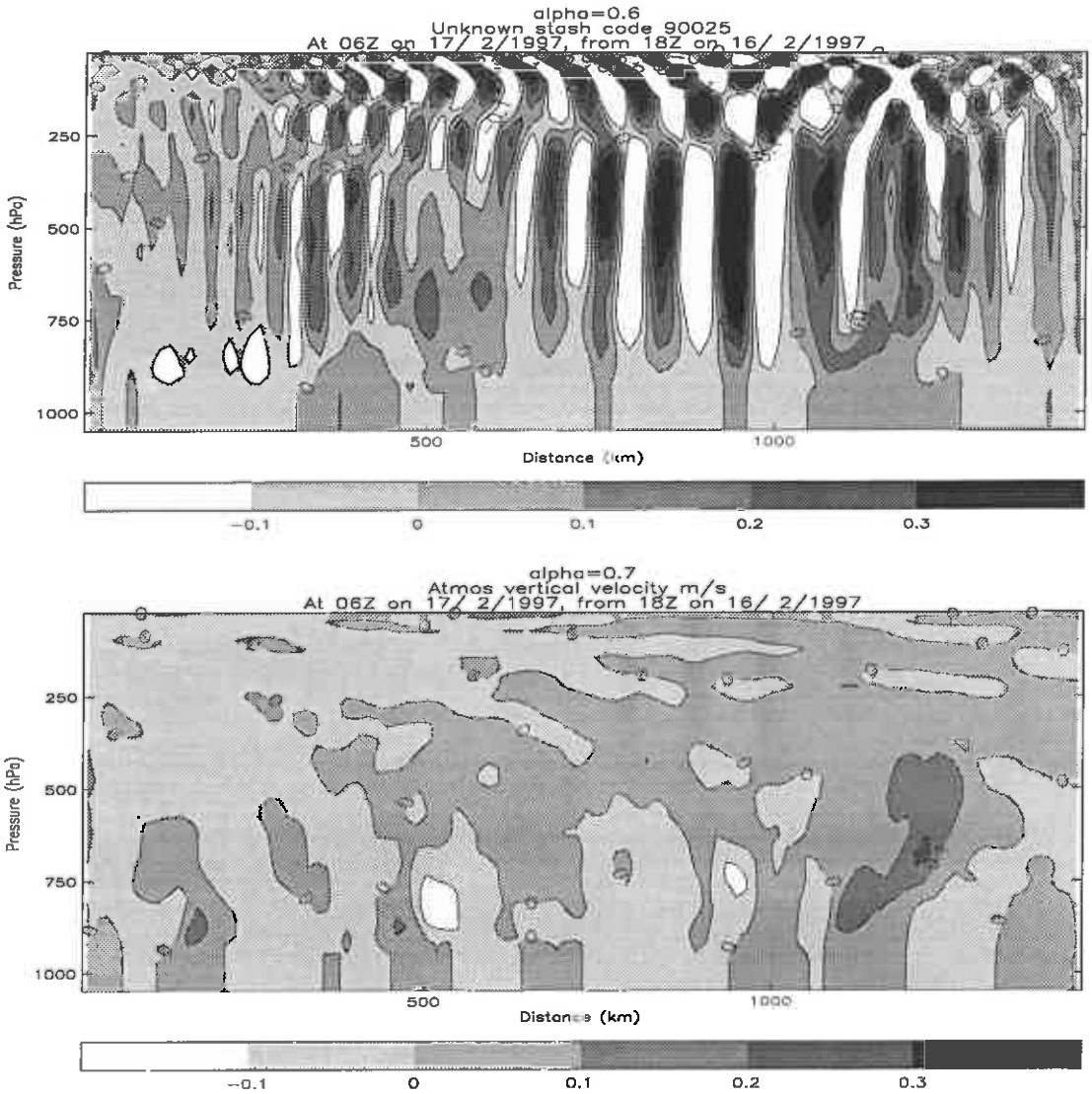

Figure 3.6 Cross sections along the line in figure 3.4 for original run, alpha=0.6 (top) compared to run with alpha=0.7 (bottom).

An oscillation which looks very similar to this has been reported by Macdonald (1999) also in a semi-lagrangian semi-implicit model in a similar case although his findings on methods for getting rid of it appear different from ours (for example it did not respond to changing the decentering). It seems likely that this problem is related to the strong jet in this case and therefore may not occur very often.

3.4 Runs with different vertical grids

In this section some reruns of the model from the 18Z 50km analysis with different vertical grids are briefly described.

3.4.1 "Option C" levels

A run was carried out with the 38 "option C" levels which is a quadratic based smooth set of levels (Terry Davies). These levels are more evenly spaced in height rather than pressure which is expected to be preferable for a height based model.

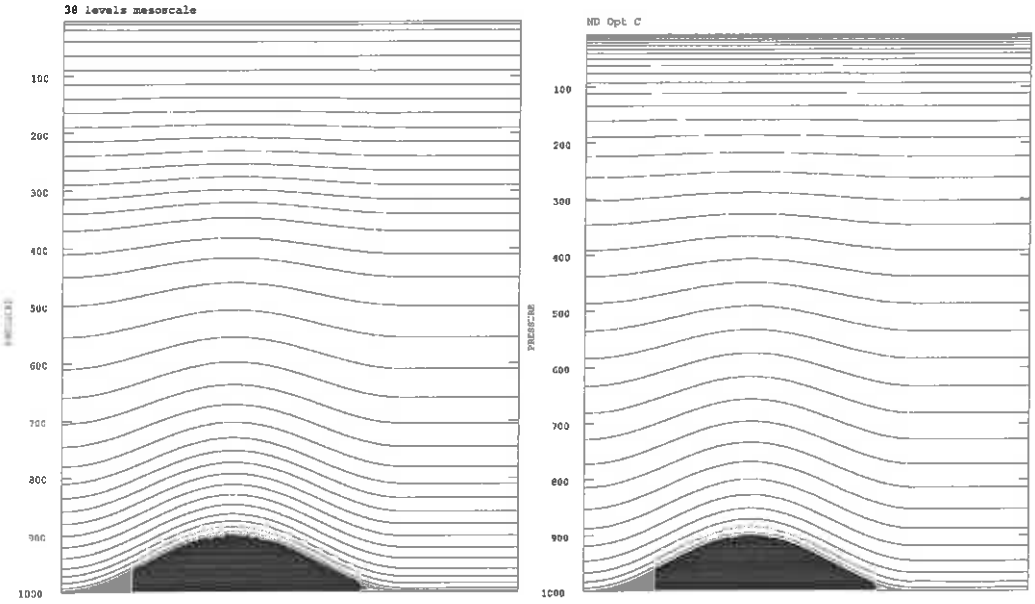

Figure 3.7 Comparison between std mesoscale 38 levels and "option C" levels.

This means in practice that the vertical resolution is increased at the top of the model, is about the same in the mid troposphere but is somewhat reduced in the lower and upper troposphere. A comparison between the two sets of levels is shown in figure 3.7. An example of the comparison between the two runs is shown in Figure 3.8.

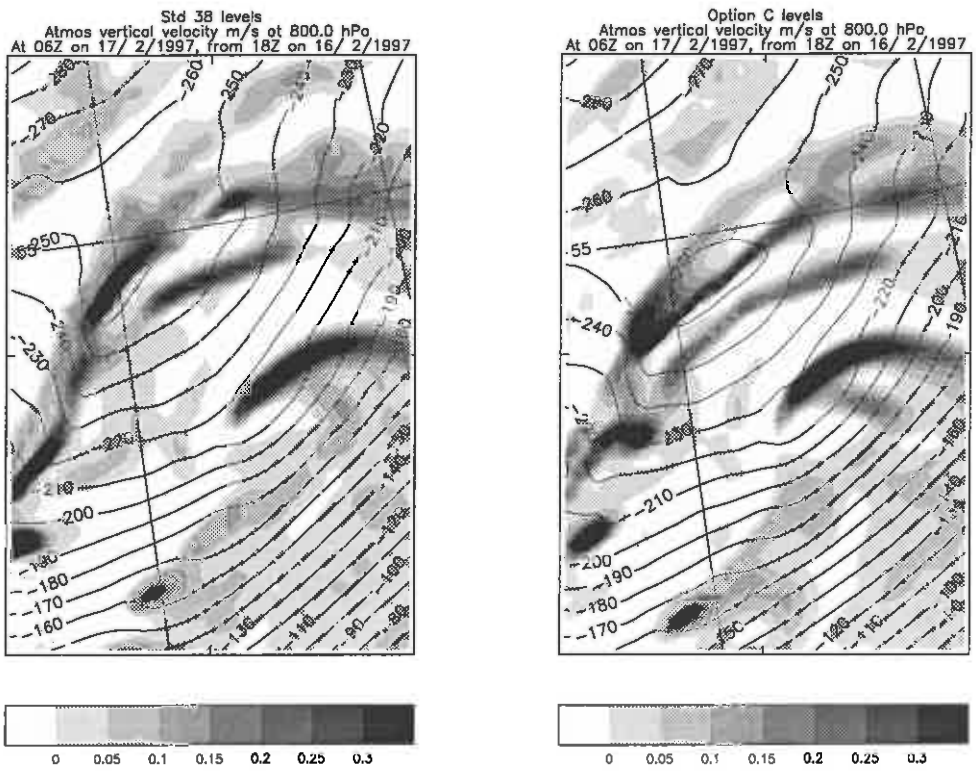

Figure 3.8 800hPa vertical velocity (shading) and 1000hPa height (contours) for t+12 forecasts for runs with std and option C sets of 38 levels.

The vertical velocity fields may be seen to be broadly similar between the runs i.e. the major fronts are in the same places. There are, however, significant differences in the smaller details. No comparison of cross sections is shown since it is hard to find a representative one. In some places the lower level vertical velocity appears to be enhanced relative to mid levels and in others the opposite is the case. There is no discernible pattern in these differences. The overall conclusion is that changing to a more even set of levels has a relatively small impact in this case but the differences that are observed are not easily explainable.

3.4.2 45 levels

In the UM work on this case the best representation of the mesoscale structure was obtained by using 45 rather than 38 levels with the extra levels used to produce a more even and smaller spacing in the mid troposphere (around 600hPa) where the 38 level resolution falls to over 50hPa. An approximation to the UM 45 levels was produced for the New Dynamics by using a stretched quadratic grid (stretched in order to avoid too many levels being put in at the top of the model). This set of levels gives higher vertical resolution than the 38 level set everywhere below 350hPa.

When the 45 level model is run from the same 18Z 50km starting point as the 38 level model significant differences are seen in some of the fields. Figure 3.10 shows that the T+12 800hPa vertical velocity field looks significantly different in that the maxima along the fronts appear weaker and less coherent in the developing system (the figure shows the field at 6Z but these differences are representative of all times from 0Z to 12Z). In contrast the front ahead of the system associated with the parent low (not visible in the figure) does not appear greatly changed.

Figure 3.11 shows a cross section along the line shown in figure 3.8 showing cross frontal slantwise circulations which are discussed in section 4.1. The two figures do not appear as different as it appears in figure 3.8. In both models the slantwise circulations may be seen. The biggest difference is that the peaks at 800hPa are no longer present in the 45 level model.

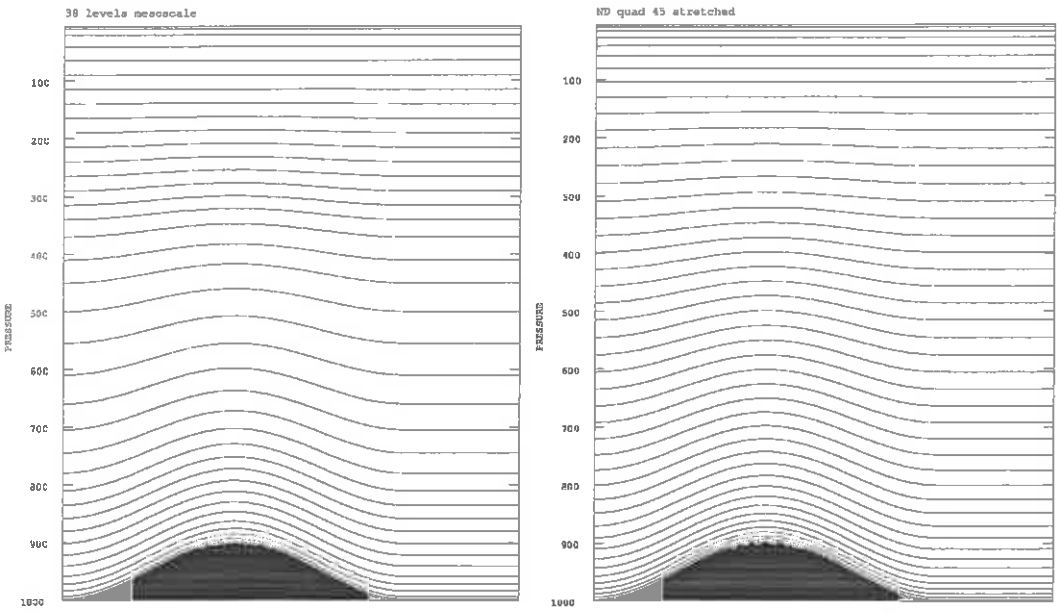

Figure 3.9 Comparison between std mesoscale 38 levels and New Dynamics 45 levels

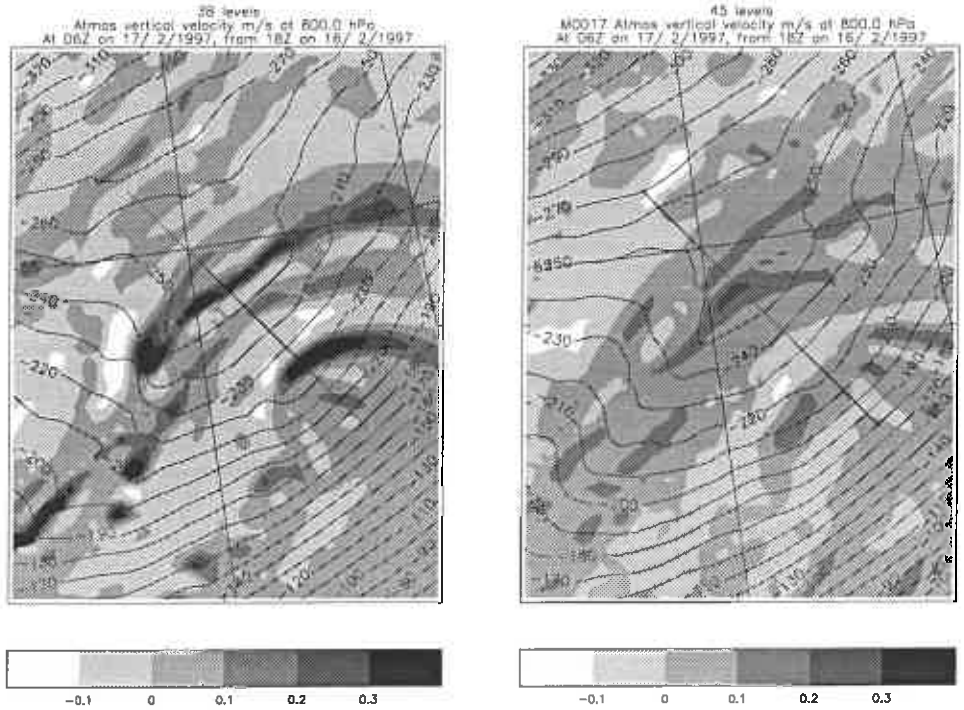

Figure 3.10 800hPa vertical velocity for 38 level and 45 level model for 6Z (T+12)

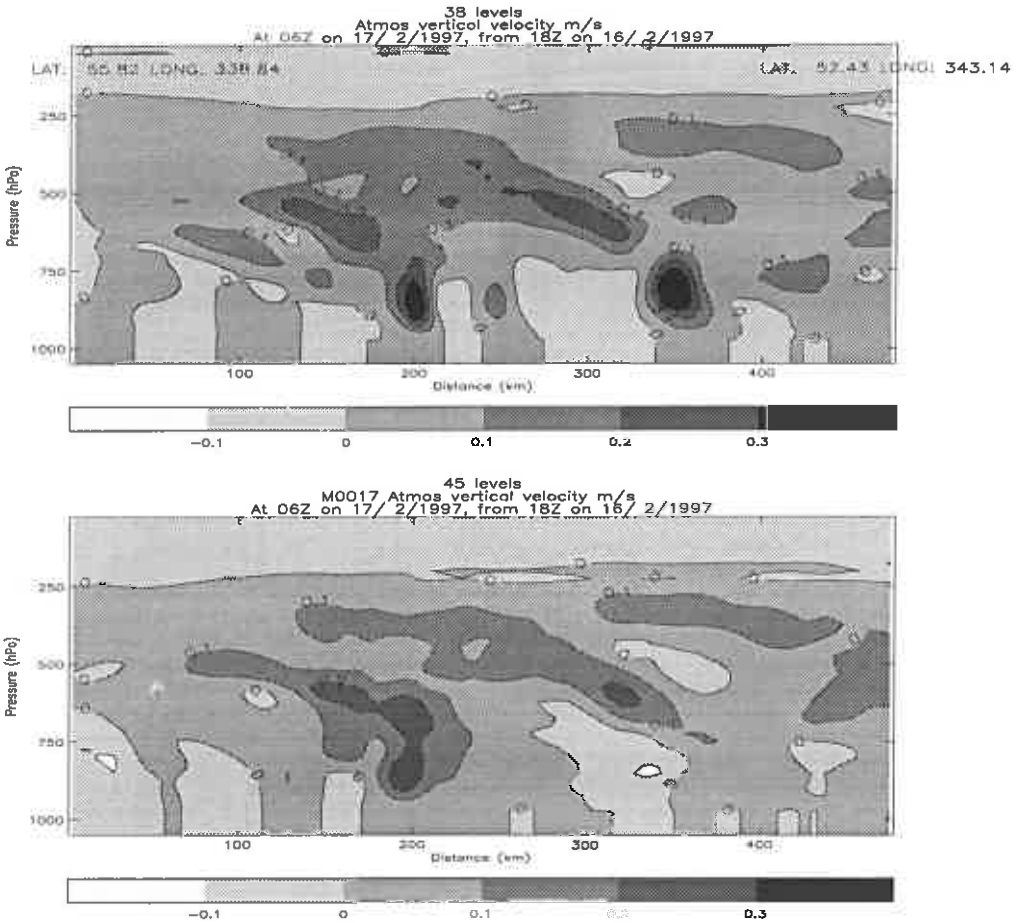

Figure 3.11 Cross Sections of vertical velocity along line in fig 3.6.

This is not a general feature since it will be shown in the next section that the 45 level model started from a mesoscale analysis does still have the maxima at 800hPa. The reason for the difference in this case is not clear. One suggestion was that the higher resolution model is resolving a thin stable layer which is not present in the 38 level one. Investigation shows that there is indeed a thin stable layer at around 750-800hPa which appears somewhat stronger and more coherent in the 45 level. Tephigrams from the two runs are shown (taken from a point just south of the southernmost front) in figure 3.12 (a) and (b). The 45 level run clearly shows a stable layer around the 0°C isotherm which is completely absent in the 38 level run. Attempts were made to investigate the cause of this difference and how it is related to the differences observed between the vertical velocities in the two runs. The 45 level model was rerun reducing the rate of or completely removing various microphysical terms in order to remove this stable layer. It was found that in order to completely remove it it is necessary to remove the melting, deposition and riming terms – the tephigram from such a run is shown in fig3.12 (c).

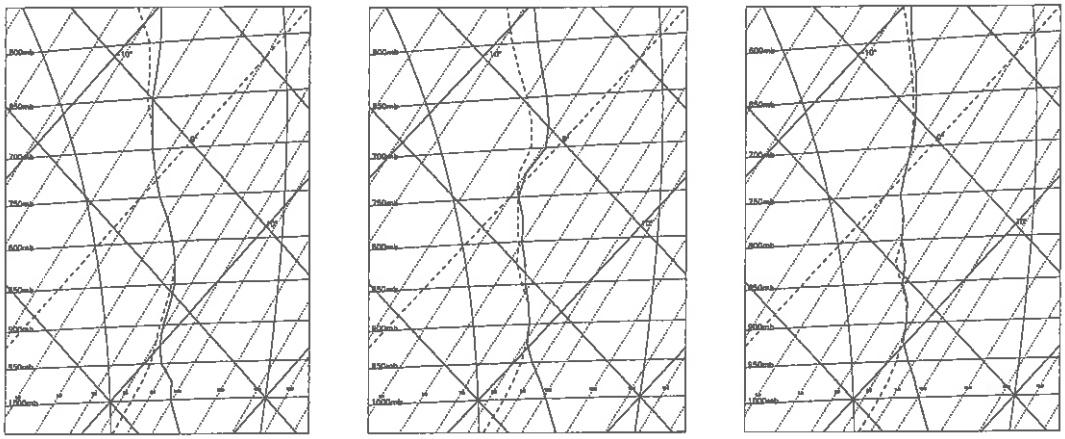

(a) (b) (c)

Figure 3.12 Tephigrams for 38 level run (a), 45 level run (b) and 45 level run without deposition or riming.

However when the vertical velocities from this run are compared to the other two it is found that it is very similar to the other 45 level run (i.e. the vertical velocities are still very weak at 800hPa). This implies that the stable layer is not the prime cause of the differences between the 38 and 45 level runs. Another aspect noticable in the tephigrams shown in fig 3.12 that the 38 level model has an unphysical looking unstable layer below the 0°C isotherm – the reason for this is not known but it is not present in the 45 level model.

Another suggestion is that the difference between the two runs is related to differences in the behaviour of the convection scheme between the two sets of levels. The differences between the two models first appear at about 0Z (T+6) and are largest around 3-6Z after which the runs tend to become more similar again. However it is noticeable that there is a larger area of convective rain around the area of the southern front at 21Z (figure 3.13).

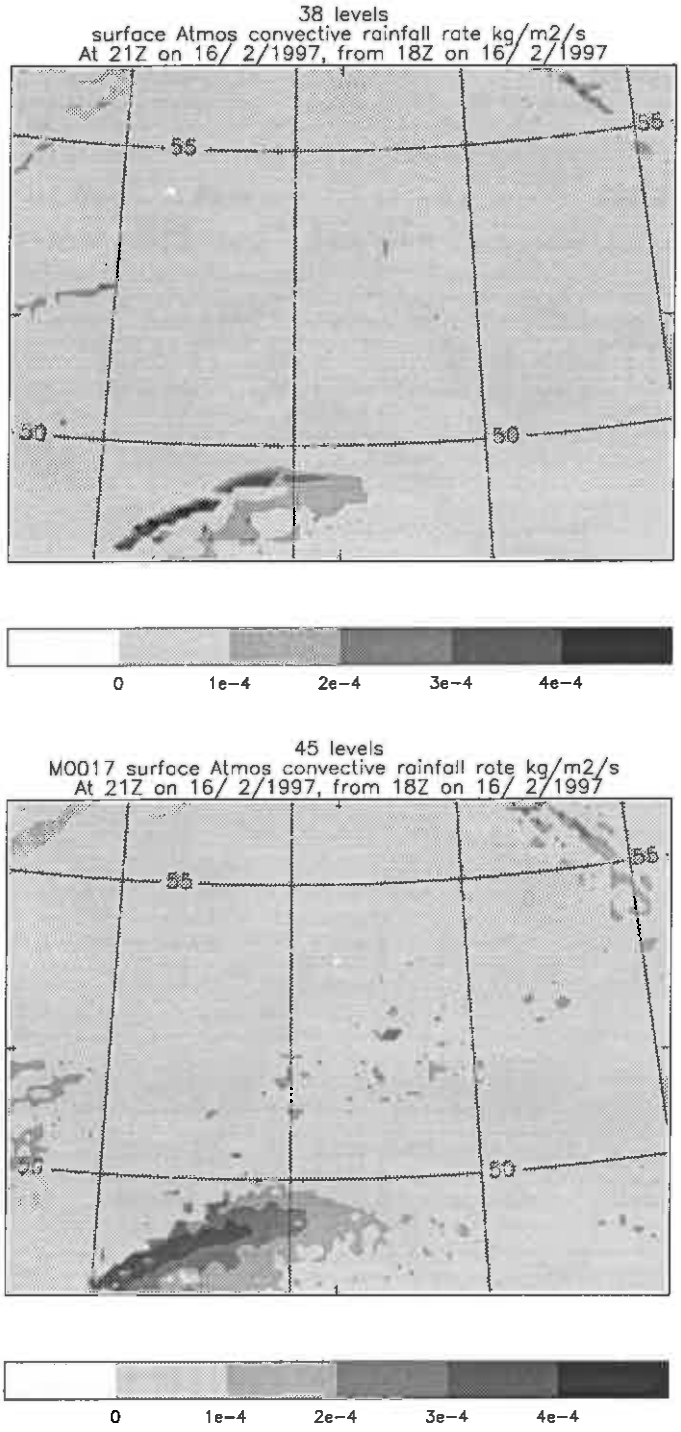

Figure 3.13 Convective rain rate for 21Z (T+3) for 38 level (top) and 45 level models over subdomain of model. Note enhancement in 45 level model near bottom left of figure area.

In order to test this hypothesis the 45 level model has been rerun with convection suppressed by increasing the CAPE closure timescale. Figure 3.14 shows that this change increases the 800hPa vertical velocity peaks. This suggests that the idea that the convection scheme is responsible for the differences may be correct.

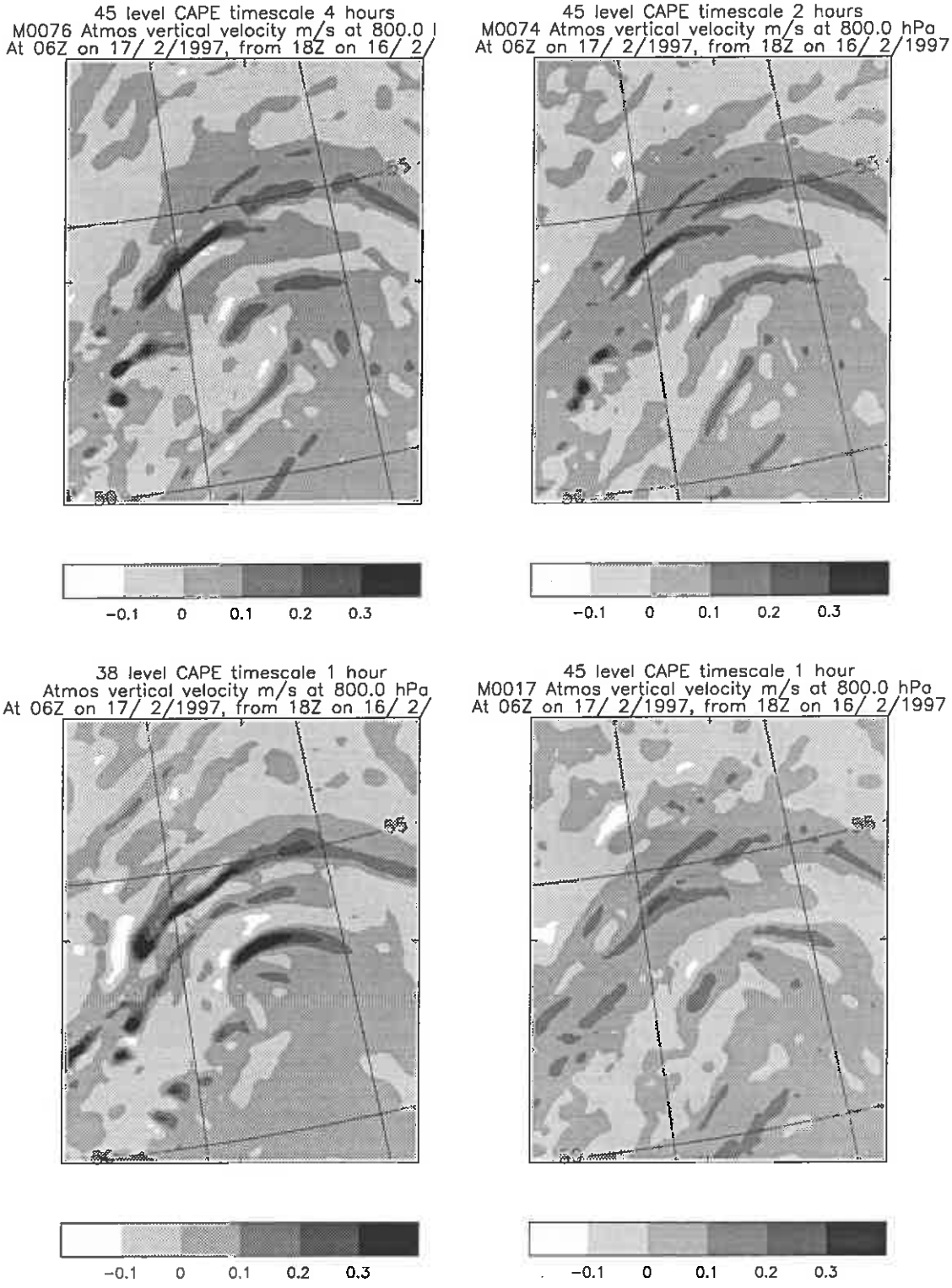

Figure 3.14. 800hPa vertical velocity at 6Z for 38 level run and 45 level runs with changes to CAPE timescale.

4. 12km Runs from 12km analysis. More detailed comparisons to UM and to observations

4.1 12km, 45 level runs from 12km analysis and comparisons to UM

The reruns in the last section initiated from the 18Z 16th 50km analysis do not represent the "best" forecast of the system in terms of agreement with observations. The previous work on the UM representation of this case (Forbes et al 2000b) found that the better model forecasts in terms of RMS errors from observations, low position and depth and observed mesoscale structure were obtained starting from a mesoscale (12km) analysis at 0Z 17th. This analysis was obtained by running the UM at 12km resolution with assimilation for 15 hours starting with a 50km analysis at 9Z 16th.

It was decided to reproduce these runs as closely as possible with the New Dynamics in order to allow a meaningful comparison with observations. The run was initialised from the UM 12km 0Z 17th analysis. It would clearly have been better to run the New Dynamics for 15 hours with assimilation to reproduce what was done with the UM but this is the best which can be done given the current lack of assimilation in the New Dynamics. The comparisons presented below are therefore expected to favour the UM in that both models were started from a UM analysis. The boundary conditions were again obtained from a (New Dynamics) global run which, in order to reduce mismatch, was started from an analysis with the 12km analysis interpolated to global resolution and transplanted into the global analysis. The model was run with 45 levels (as shown in figure 3.5(b)) since this is what was done with the equivalent UM work.

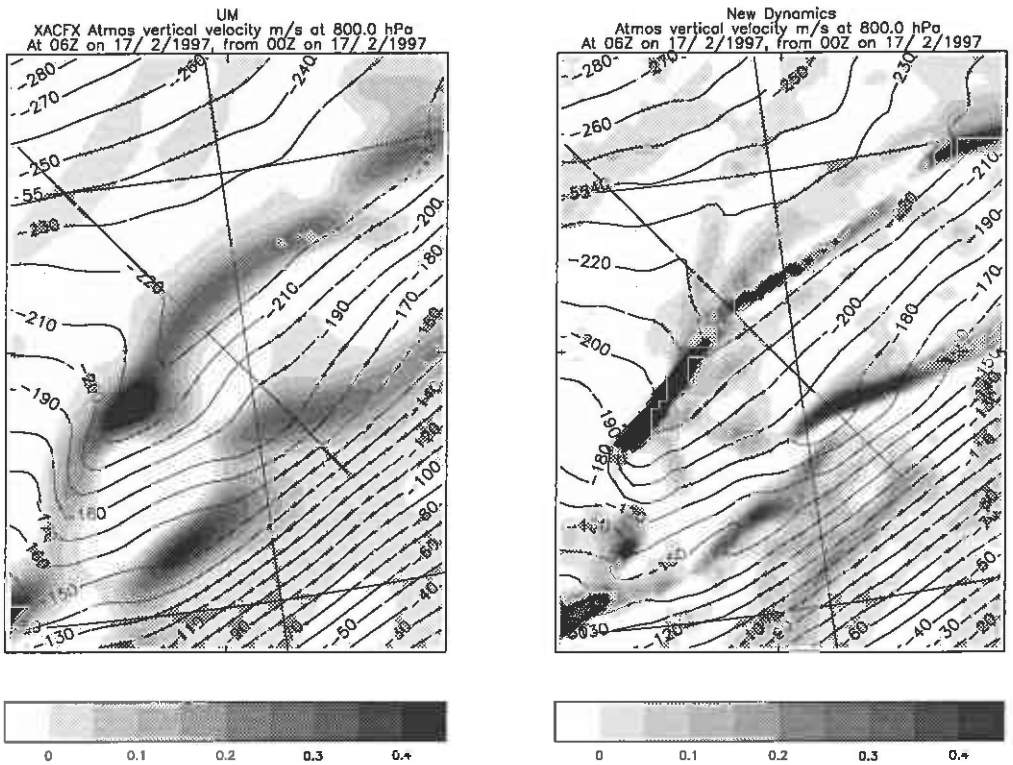

Figure 4.1 800hPa vertical velocity (shading) and 1000hPa geopotential height for UM and New Dynamics at 6Z 17th (T+6 forecast)

Figure 4.1 shows the T+6 800hPa vertical velocity fields and showing the double frontal structure. The primary conclusion, that features are much sharper in the horizontal in the New Dynamics, is clearly valid in these runs as well as in those described in section 3. This sharpening is also reflected in the maximum values of 800hPa vertical velocity along the front which are approximately 0.8m/s for the UM runs and 1.5m/s in the New Dynamics model.

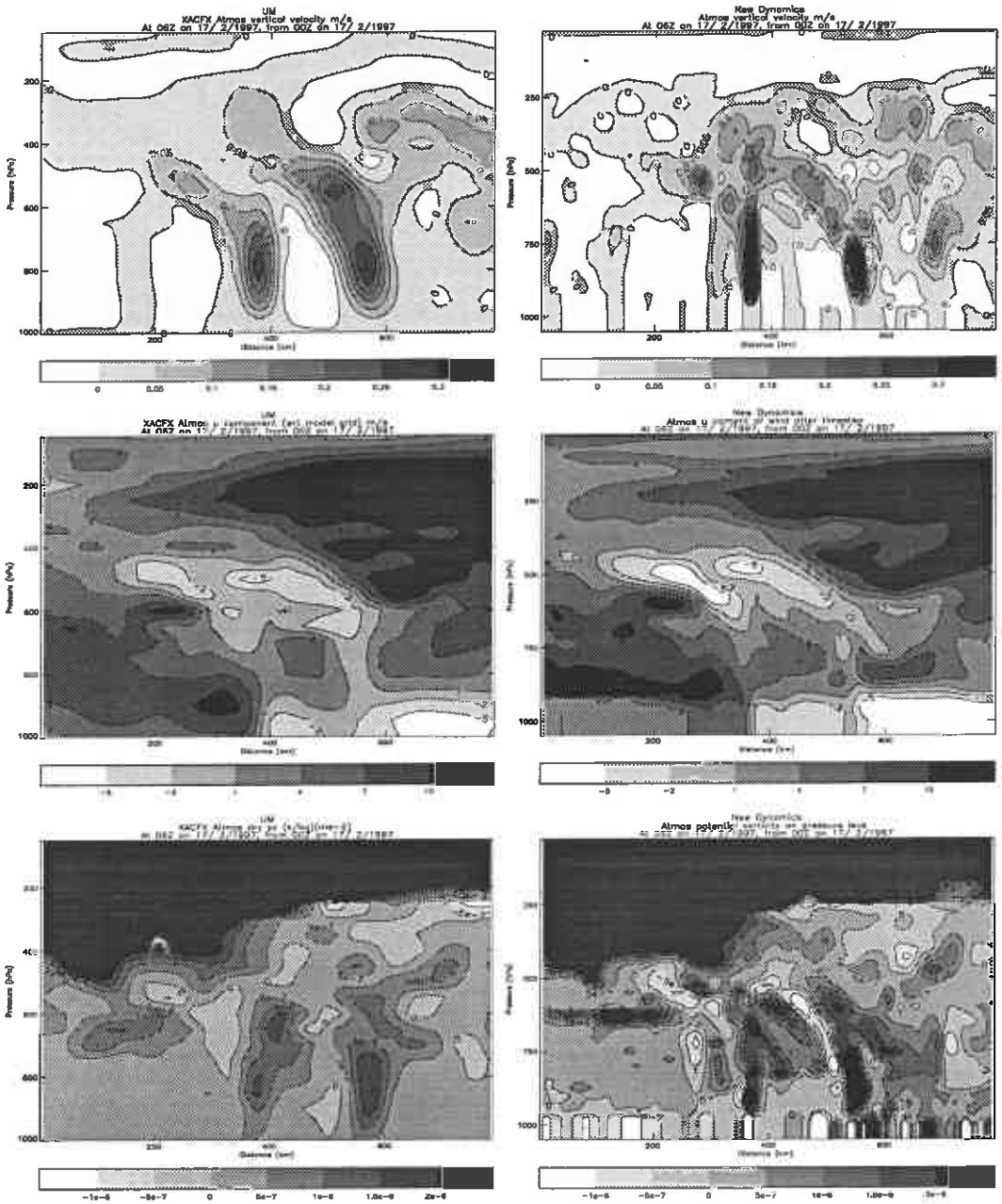

Figure 4.2 Cross sections of Vertical velocity, Cross frontal velocity and PV for UM and New Dynamics at 6Z (T+6). Note that the area at the bottom of the New Dynamics sections characterised by vertically oriented contours is below the ground.

Figure 4.2 shows a number of cross frontal cross sections along the lines in figure 4.1. These cross sections show the cross frontal slantwise circulations associated with the two fronts which are discussed in some detail in Forbes et al (2000b). The vertical velocity cross section brings out the slantwise structures clearly. The features are sharper in the New Dynamics the narrow, vertical maxima centred on 800hPa are suggestive of line convection in this run. The vertical velocity maxima along the slantwise portions of the flows is more broken up in contrast to the cross frontal velocity which shows more coherent, shallower flows in the New Dynamics which intuitively look more realistic. The PV cross sections clearly show multiple tropopause fold structures in both runs with peaks of positive diabatically generated PV in the regions of strong ascent and negative PV being advected along the circulations. These features are again much sharper in the New Dynamics and (as might be expected from the fact that the fronts have collapsed further) the values of PV observed are more extreme.

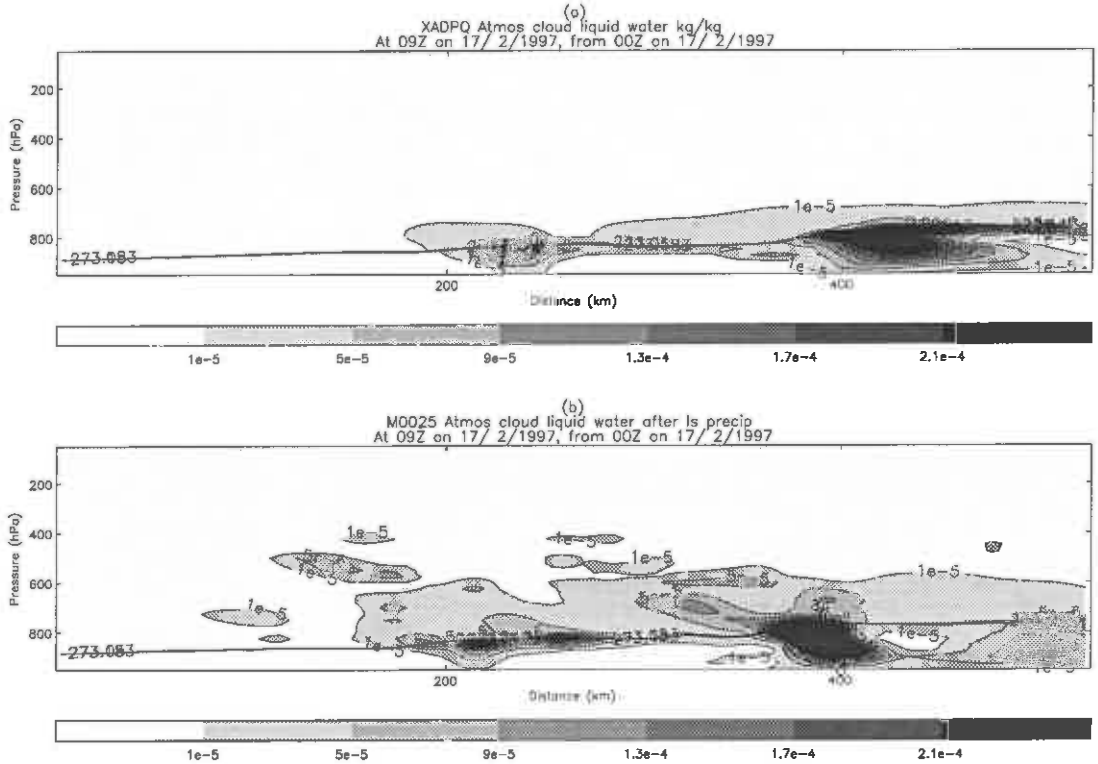

Figure 4.3. Cross section across the fronts at 9Z (T+9) showing cloud water (shading) and melting level (contour) for (a) UM and (b) New Dynamics

The cloud ice is broadly similar between the UM and New Dynamics (figure4.7) – as would be expected from the above there is somewhat more variability in the ice fields in the New Dynamics model but the overall values are similar. There is more difference in the cloud water fields. As may be seen in figure 4.3 there is considerably more cloud water above the melting level in the New Dynamics model than in the UM. The reason for this is not known and will be the subject of future work.

4.2 Comparison to Observations

We have seen that the results from the New Dynamics runs look very different from those from the UM and often intuitively look better. It is therefore important to compare the results from both runs with observations to verify which is producing results closest to the real case. This section describes the attempts to do this.

4.2.1 I R Imagery

Figure 4.4 shows a comparison between model cloud top temperature fields and the IR imagery. The model cloud top temperature was calculated simply by searching

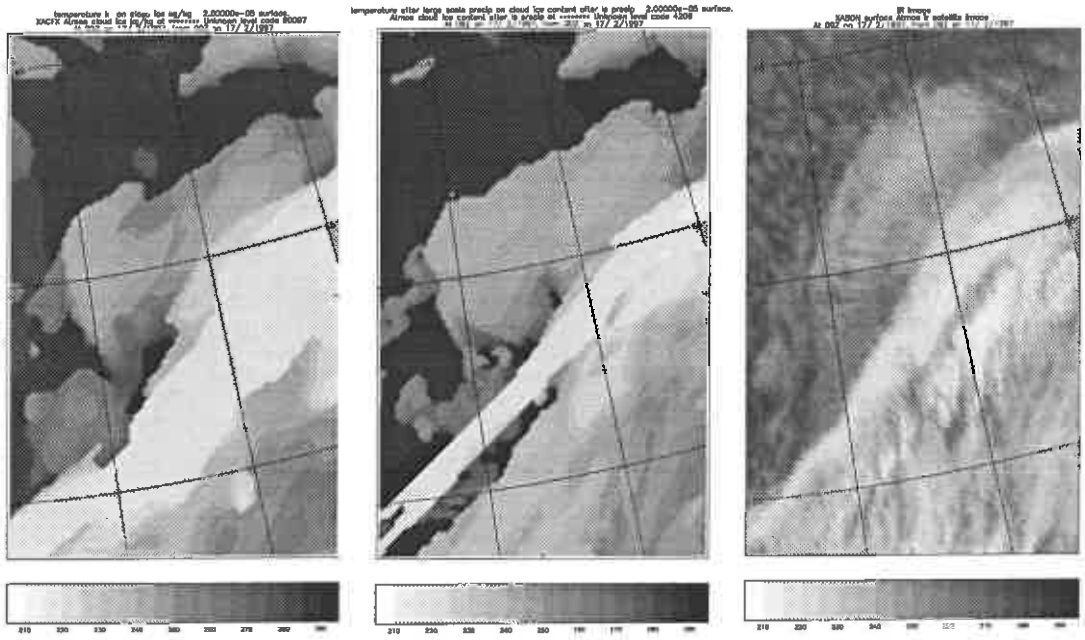

Figure 4.4 Cloud top temperature fields for UM (left) and New Dynamics (centre) compared to satellite IR image.

down for a threshold ice value of 2.0×10^{-5} g/g and plotting the temperature at that value (the threshold value used was chosen to make the images look similar to the top of atmosphere outgoing LW diagnostic). The twin cloud heads may be seen emerging from under the cloud shield. As might be expected, the two model runs have many errors in common when compared to the imagery. For example the cloud heads are over developed, the rearmost cloud head is more developed than the forward one and the dry slot is also too pronounced. Both models have fields which are rather smooth compared to the imagery although, as might be expected from what has already been shown, the New Dynamics is somewhat less so. One aspect which appears better in the New Dynamics run is that the cloud shield weakness parallel to the cloud edge evident in the imagery appears in the New Dynamics but is not as clear in the UM (although it should be noted that this feature does appear in some UM runs also).

There are also north-south running features in the cloud shield which are hinted at in the New Dynamics but not the UM.

4.2.2 Dropsondes

This section discusses comparison of the two models to data from the dropsondes released by the UK C-130 aircraft between 6 and 12Z on the 17th. Table 4.1 shows the RMS error of three quantities between the model runs and the sondes at all levels.

	Temp RMS error (K)	RH(ice) RMS error (%)	U,V magnitude RMS error (m/s)
UM	1.96	27.8	5.98
New Dynamics	1.91	25.5	5.91

Table 4.1 RMS Errors for model runs compared to dropsondes

The table shows that for all three quantities shown the RMS error is less for the New Dynamics run compared to the UM. The difference ranges from about 10% down to about 2% but this is quite encouraging when it is considered that the New Dynamics fields have a good deal more short range structure. Normally a run with more short range structure would be expected to have a higher RMS error due to the larger effect of random errors or phase errors of features. During the UM work (see, for example table 3.2 of Forbes et all (2000b)) it was found that the 50km run had the smallest RMS error simply because the fields were so smooth. The fact that the RMS error for the New Dynamics is smaller may therefore imply that the New Dynamics run is in substantially better agreement with the observations.

A second approach with the dropsondes is to compare objectively analysed cross sections from the various aircraft runs through the system with the model cross sections. The objective analysis technique attempts to take the dropsonde data from each aircraft run and produce a best estimate of the corresponding cross section of the observed and derived fields. More details of this may be found in Forbes et al (2000a). The cross sections shown in the report were analysed on theta surfaces. An example of an attempt to compare the models to these sections is shown in figure 4.5.

As in the previous section it is clear that the model runs are more like each other than the observations although obviously some of the gross features are similar but displaced (no attempt has been made to correct the position of the cross section for positional errors in the model). From the density of the sondes in the sonde cross section and the general smoothness of the fields it can be seen that the major problem is that the sondes are too far apart (at least 60km) to verify a model at 12km resolution.

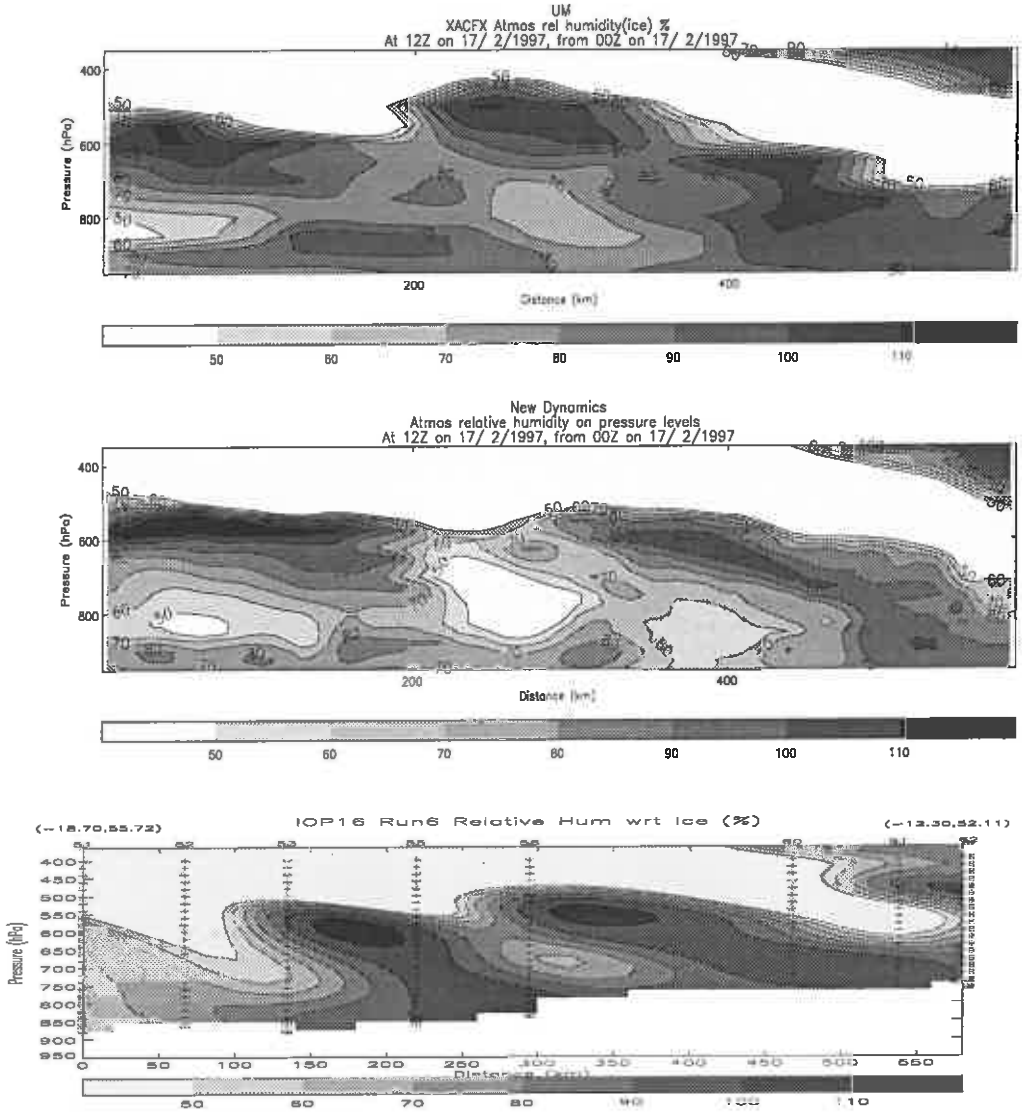

Figure 4.5 Relative Humidity cross section corresponding to aircraft run 6 from UM (top), New Dynamics (middle) and objectively analysed from dropsonde data. The vertical lines made up of crosses in the dropsonde cross section indicate the positions of the sondes.

4.2.3 P-3 Radar

In this section the radar data from the NOAA P3 aircraft is discussed. This aircraft closely followed the track of the C-130 aircraft and made a number of cross frontal runs through the system. Figures 4.6 and 4.7 show a comparison between the radar reflectivity and the model calculated reflectivity for one of the runs through the system.

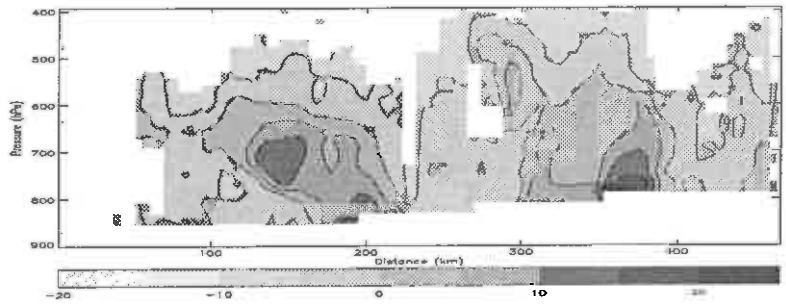

Figure 4.6 Radar reflectivity for run 1

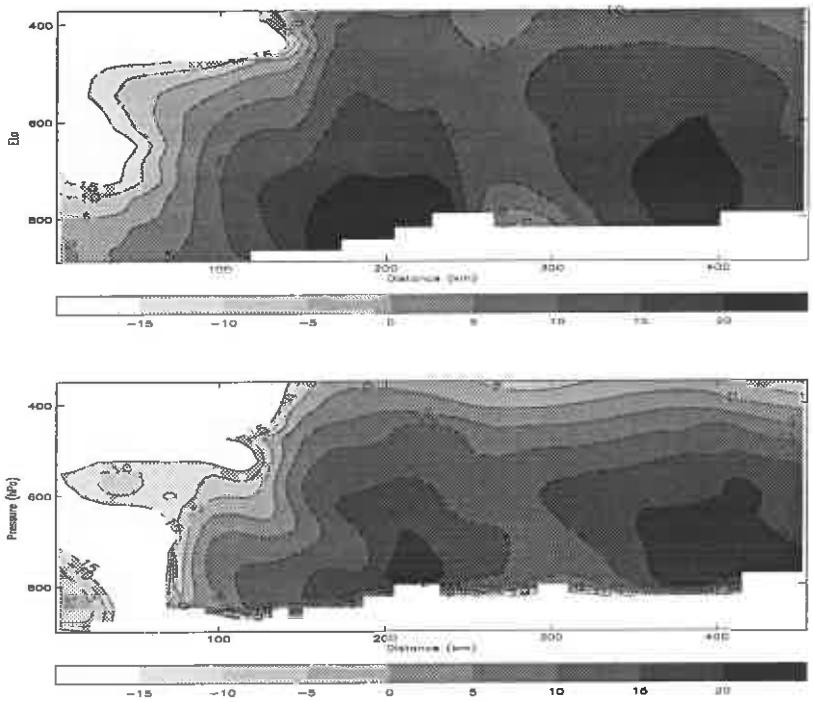

Figure 4.7 Model cross sections of reflectivity (above freezing level only) for run 1 for UM (top) and New Dynamics.

The reflectivity is dominated by ice particles above the melting layer and rain drops below. Since the rainfall on model levels is not currently available for the New Dynamics we can only make a comparison above the melting level. The reflectivity's shown in figure 4.7 are calculated by making microphysical assumptions consistent with the model microphysics. There is some qualitative agreement between the model and the radar in the sense that the two frontal peaks with signs of slantwise ascent can be seen in both The overall values of reflectivity are however around 5dB higher in the model than in the observations implying that the model has too much ice. The model reflectivity appears somewhat smoother than that observed – it is clear that in both model runs the variability of the ice field in the horizontal and vertical is too small. The new Dynamics run does looks somewhat less smooth than the UM but is still smooth compared to the radar.

A similar conclusion can be drawn from looking at horizontal fields extracted from the radar dataset compared to corresponding model fields – once again the model ice fields are much smoother than the radar data. An important question to investigate in the future is the reason why this is the case.

4.2.4 Land Based Radar

Towards the end of the period of interest (9-12Z) the bands of rain in front of the system crossed the northern UK and Ireland. It was therefore decided to compare the model rainrates with those from the land based radar network. This comparison is shown in figure 4.8 and 4.9.

It is immediately obvious that the usefulness of this comparison is very limited by the fact that the main rainbands in the system (i.e. those associated with the two fronts) do not cross the radar network during the period of the model runs. There is, however, clearly some agreement between the models and the radar with rain ahead of the system over the west coasts of Ireland and Scotland/England with a gap between (over eastern Ireland and the Irish Sea). Once again both model runs appear rather smooth compared to the radar although the New Dynamics is significantly better in this regard. The New Dynamics appears preferable in this case in that there is less orographic enhancement over the southern tip of Ireland which is not at all evident in the radar data. However it is hard to conclusively say that the New Dynamics model is better from this comparison.

4.2.5 SSMI data

Attempts were also made to verify model runs again the SSMI rainfall data which is available for the period. This comparison has yielded virtually nothing due to the low resolution of the available SSMI data (about 50km).

4.2.6 Conclusions on Comparison of Models to Observations

The conclusion of this section is that the New Dynamics model doesn't appear to be worse than the UM in terms of agreement with the observations. So far, however, it is difficult to show that the New Dynamics model is better. The statistical comparison of the RMS errors in the two models to the dropsonde models is suggestive that the New Dynamics is in better agreement. The fact that the New Dynamics has more short range variability clearly makes it look more like the radar data than the UM although there is still nothing like as much variability in the model ice fields as one might hope for.

More work needs to be done on this particularly to ascertain if more can be gleaned from the P3 radar data which is in the course of being reanalysed by the group at CETP.

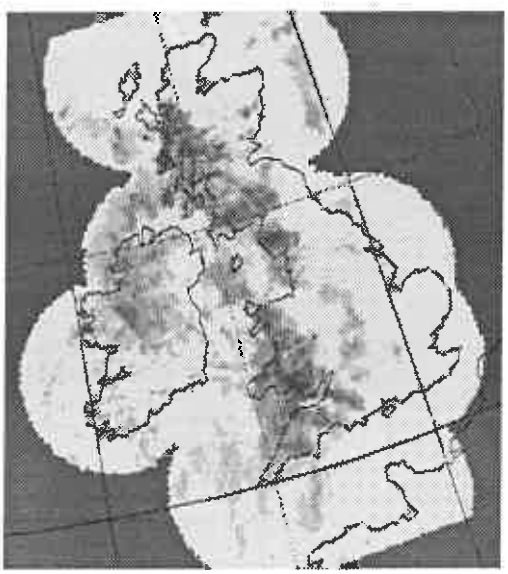

Figure 4.8 Rainrate for 12Z 17th from rainfall radar (left), UM (middle) and New Dynamics (right).

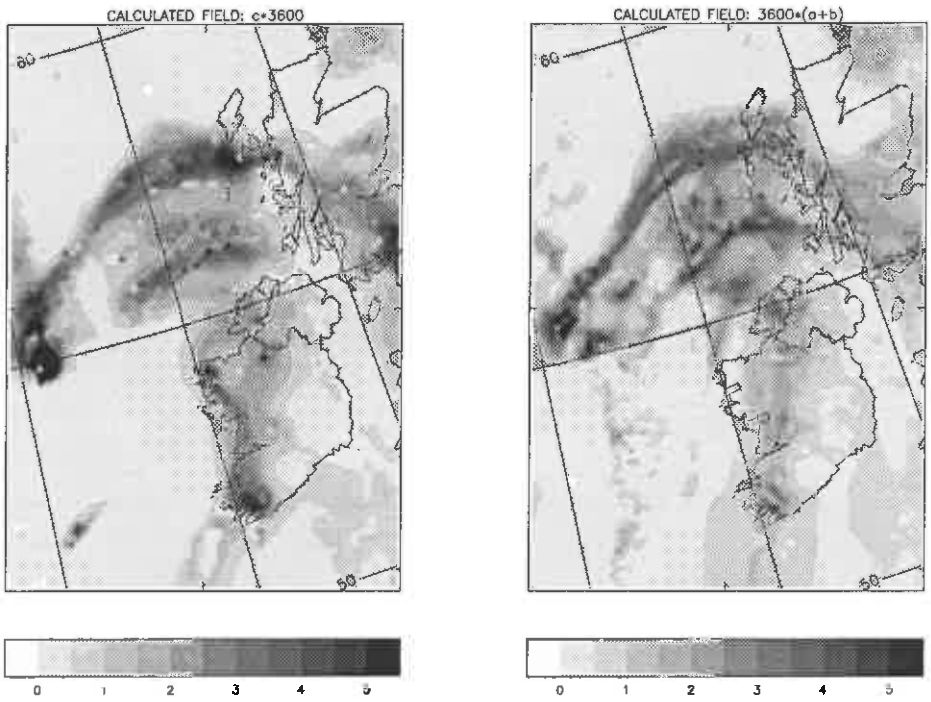

Figure 4.9 Rainrate for 12Z 17th form UM (left) and New Dynamics. Scales are approx. same as fig 4.7

5. 4km Simulations

In this section the results from running the model at 4km resolution are discussed.

5.1 Overview

The model was run over a 394x247 point domain at 0.035° (approximately 4km) resolution which was (one way) nested within the 12km model so as to give a domain extending approximately 1600km west from the W coast of Ireland (figure 5.1 shows the whole domain of the model). The domain was chosen in order to keep the system within it for as long as possible. It is as large as can be practically used with current computing resources (having about as many 3D gridpoints as the current operational global model). The model was run with the same 45 level set as the 12km runs discussed in section 4 (figure 3.5 (b)). As will be discussed later this may not be sufficient levels for this resolution but it was the easiest thing to try since vertical interpolation for producing boundary conditions is not currently available within the New Dynamics and, anyway, may not be desirable. The model was initially run with a 2 minute timestep, no diffusion except on the top two levels and a CAPE closure timescale of 20 mins.

The first attempts to run the model on this domain threw up a number of problems which are discussed in section 5.2. In the rest of this section an overview of the results after these problems were resolved is given.

The 4km model 1000hPa geopotential height compared to those from the 12km run are shown in figure 5.1. The overall pattern is very similar. The main difference is that the contours are rather noisy looking in the 4km run. The fluctuations in the contours correspond to pressure changes of order 0.2mb. This, in itself, may not be a bad thing, it may be that there would be expected to be these kinds of variations in pressure at these resolutions. It is noticeable that the contours are *not* noisy everywhere, for example they are not noisy in the SE and NW corners of the domain. The noise is therefore not simply an intrinsic characteristic of the model. If the pmsl field is animated it can be seen that the fluctuations move along the isobars at roughly the advection speed which implies they may be realistic features. They appear to be associated with the convective cell like features discussed below. Even if these fluctuations are expected to be there they raise the issue of what would be done with such data when these models come into operational use – it may be necessary to smooth it for presentation and post processing purposes.

Figure 5.2 shows the 800hPa vertical velocity fields for the two models at the same time. As would be expected there is much more short range variability in the 4km model. The fronts, for example, are far sharper (in fact they are almost the same width in terms of gridpoints as in the 12km model). The fields look meteorologically reasonable overall. In the region of convection to the NW of the system there are many cells of vertical velocity which look like an attempt by the model to reproduce convection. These cells are typically 3-5 gridpoints across (*not* single gridpoints) and can be seen spinning up as the air enters the model at the western boundary. The noise in the 1000hPa geopotential height contours commented on earlier can now be seen to correspond to the region where there are all these small cells of vertical motion. There is more discussion of the representation of convection in section 5.3.2.

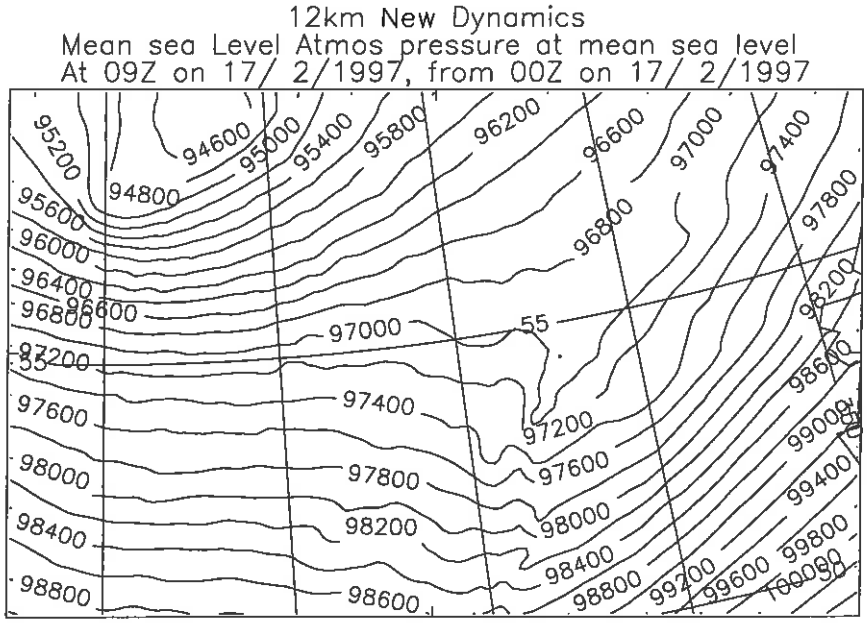

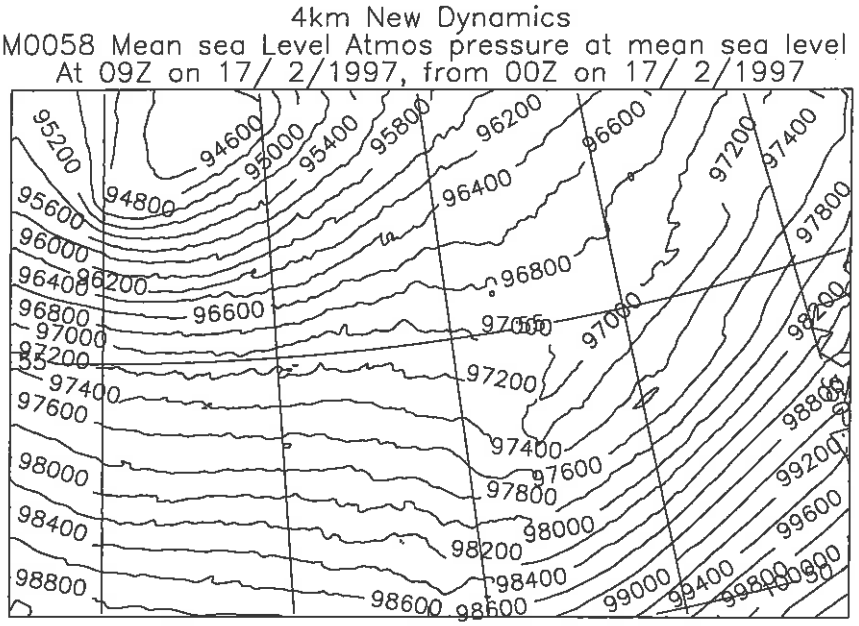

Figure 5.1 1000hPa geopotential height from 12 and 4km models over the whole domain of the 4km run (note coast of Ireland in extreme E of domain).

The values of vertical velocity which are observed are quite large, typically between 1-2m/s in the maxima along the fronts (compared to typical values of 0.5 – 1.0 m/s in

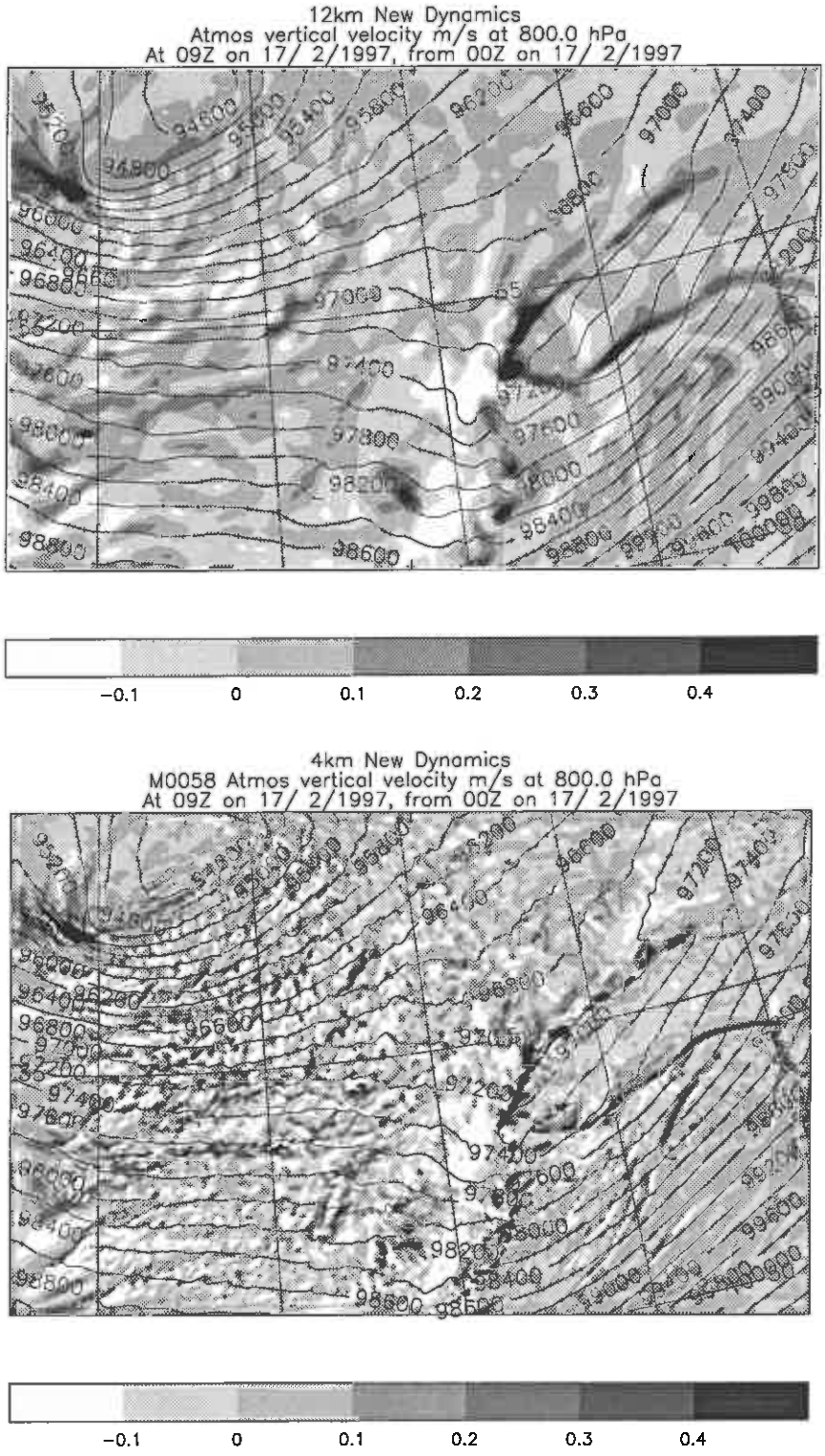

Figure 5.2 800hPa vertical velocity (shading) and 1000hPa geopotential height (contours) for 12km and 4km models.

the 12km run). The maximum values of vertical velocity at 800hPa in this run are around 6m/s which is a cause for concern since it implies that the air rises 600m

during one timestep (which is considerably further than the model level separation). This is one of the considerations which lead to the experiment described in section 5.3.1 of reducing the timestep.

In order to look in some more detail at the frontal structure some cross sections across the fronts are shown in figure 5.3. The vertical velocity cross sections show that the low level maxima have become narrower and more vertical – this looks like a more realistic representation of line convection. The region of slantwise ascent shows a break up of the slanted sheet of vertical velocity seen at 12km into individual maxima. This might be caused by the aspect ratio of the grid – i.e. more vertical levels are needed with this horizontal resolution (although it could also be real). For this reason running with more vertical levels is one of the next things which will be tried. Another general feature which is noticeable about the vertical velocity cross section is that in the 4km model there are more apparent signs of more than one circulation rather than just two although these are not evident in the horizontal velocity cross sections. These features may be convective like cells.

The cross frontal velocity component cross section shows remarkable similarity between the 12km and 4km runs. The maxima are somewhat narrower and stronger in the 4km run. The PV cross sections shows that the fields have become far more noisy at 4km resolution although the general structures are the same. As would be expected the extreme values of PV have larger magnitude. As with the vertical velocity it might be suspected that some of the breaking up of structures may be caused by insufficient vertical resolution.

Other fields of interest are the precipitation although as highlighted in section 4.2 there is a lack of validating data. Figure 5.4 shows the convective and large scale rain rate in the 12 and 4km models. The convective rainrate shows more realistic structure in the 4km run in that the scale of the cells seen in the convective region to the NW of the system looks more realistic. As would be expected from the vertical velocity data the maxima at the fronts are much narrower. The large scale rainrate is still confined to the area of the system. It is a valid question to ask why, given the vertical velocity structure seen in the convective region there is no corresponding large scale rainfall. This question has yet to be investigated.

5.2 Problems Encountered with 4km Model

This section describes two problems which have been encountered with the 4km model.

When the first attempts were made to run the model problems were encountered with the model crashing. It became clear on examining the fields output just before the failure time that, although they generally looked reasonable, a great deal of mismatch was appearing at the boundaries. First attempts to remove this problem involved trying 8 point rather than 4 point boundaries but this did not help the problem. It was soon realised, however, that these first runs used 3 hourly updating of the boundaries which was clearly not frequent enough (particularly in this fast moving case). The model was rerun updating the boundaries every hour and it ran without problems. This result is an indication that the frequency of boundary updating will be something which requires serious consideration in high resolution models. It should be remembered that at intermediate times the boundary fields are simply time

interpolated. This means that a discrete feature such as a front, moving along the boundary is not advected between update times as would be hoped for but varies between being sharp at update times and being at both positions but reduced in size half way between. The result is that in an animation a feature appears to jump between update times rather than advect smoothly. More work is required on this issue.

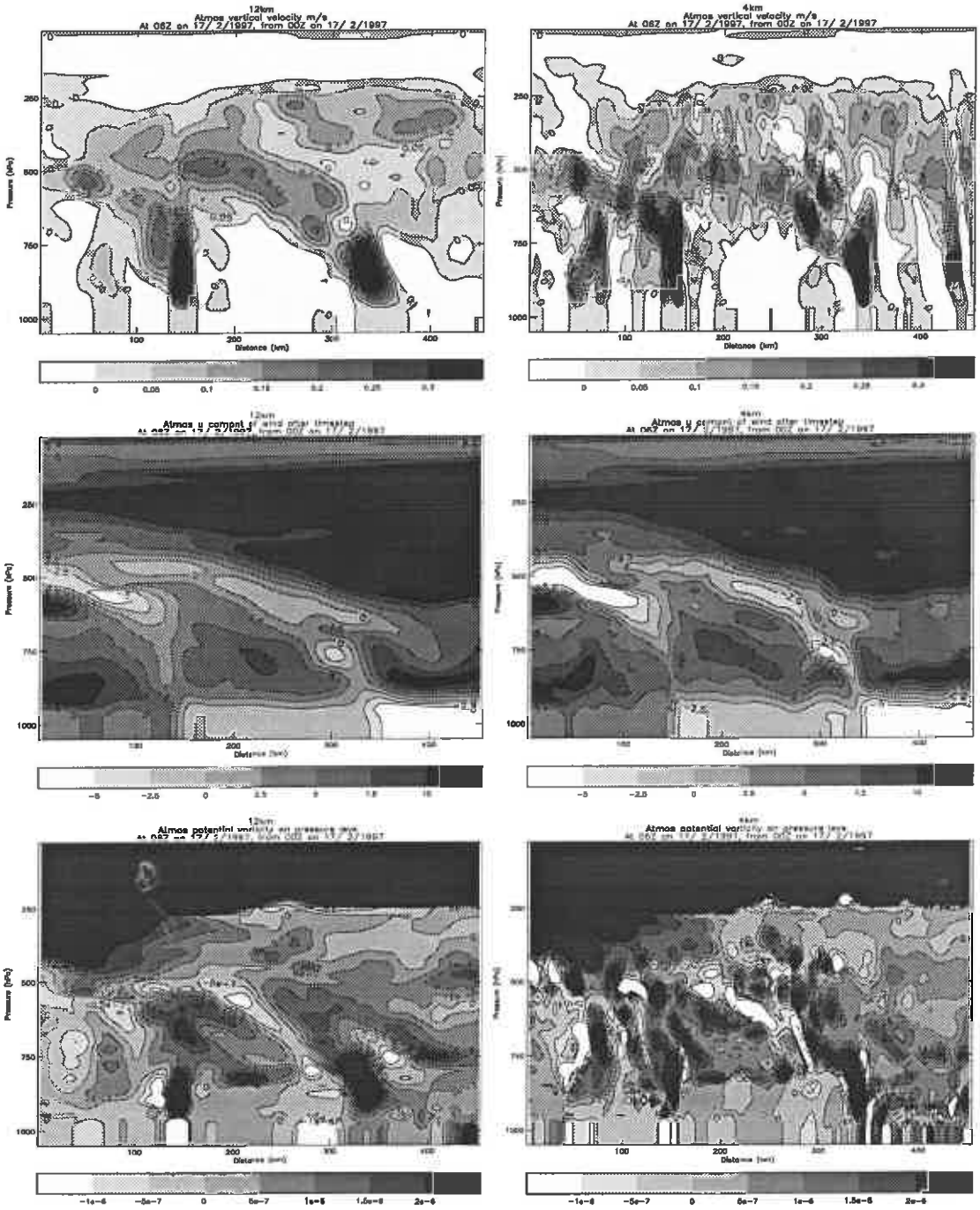

Figure 5.3 Cross frontal cross sections of Vertical velocity, cross frontal velocity and PV for 12km and 4km runs.

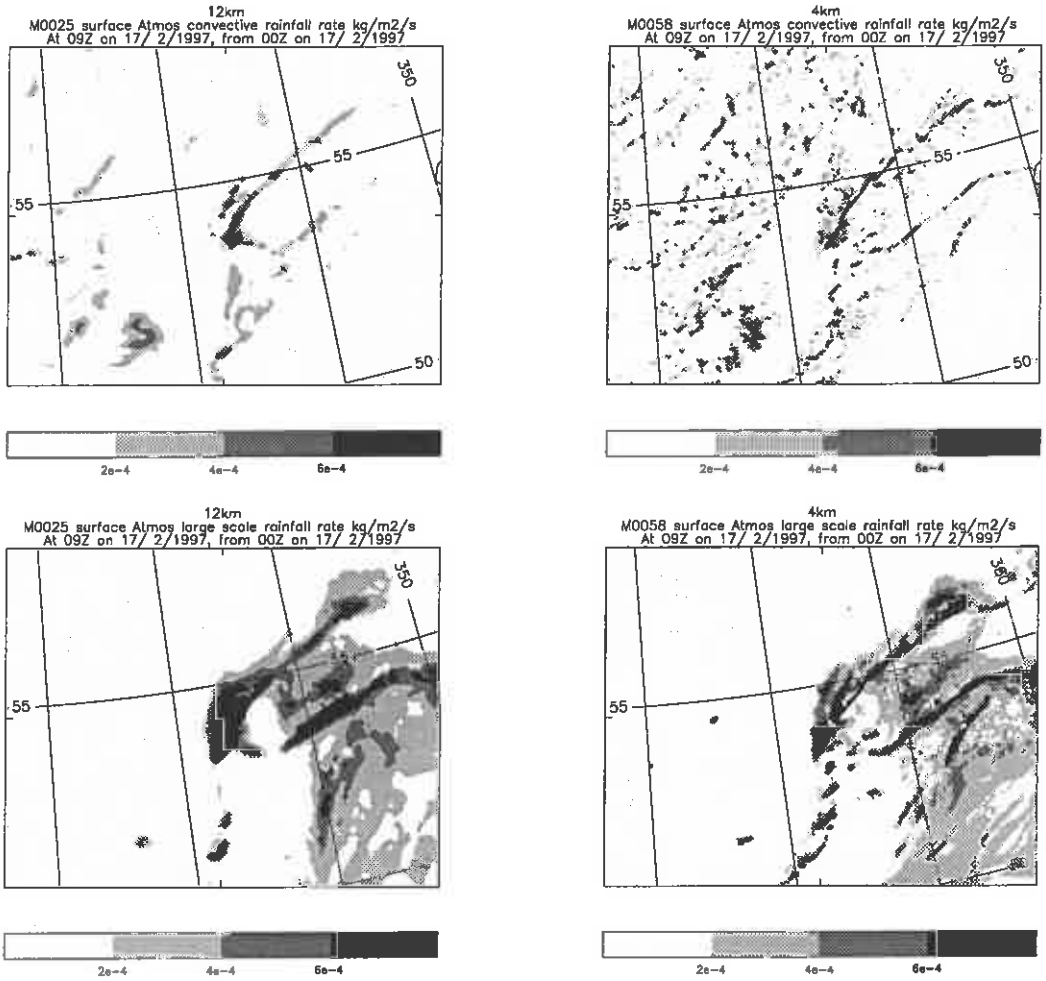

Figure 5.4 Convective and Large Scale (instantaneous) rainrates in 12 and 4km models at 9Z (i.e. T+9 forecast)

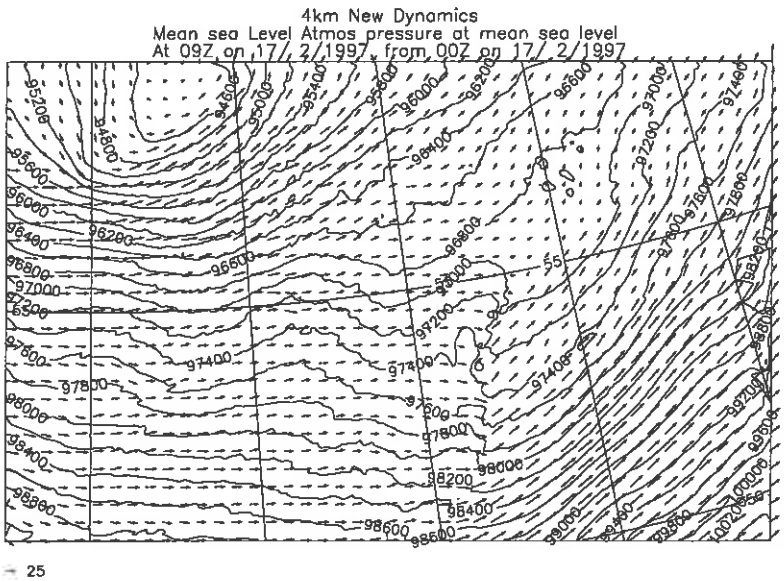

Figure 5.5 pmsl and 900hPa winds from early run of 4km model in T+9 forecast.

The second problem which was encountered is illustrated in figure 5.5. The contours show the pmsl field from one of the first successful 4km runs carried out. One feature which stands out when compared to the 12km run (figure 5.1(a)) is the broad multiple ridge/trough structure behind the system. At first this was assumed to be a synoptic feature but it was soon discovered, as shown in figure 5.5, that the winds do not flow around this structure as would be expected. An animation of this feature showed that the ridge/trough structures move along rapidly in a wave like fashion. The speed of movement is of order one wavelength of the structure (about 200km) in 20 minutes which is obviously too fast to be a genuine structure and suggestive of a sound wave in the model. This theory is backed up by the fact that the structures can not be seen in any other model field with the exception of density perturbation. This problem was eventually solved by decreasing the tolerance on the convergence of the Helmholtz solver by a factor of 10. This gave the results shown in figure 5.1(b). The implication is that the waves are a result of the Helmholtz solver having not completely converged. This is, again, a factor which needs to be optimised when specifying high resolution models given that in practice there is a trade off between cost and accuracy.

5.3 Comparison to Observations

In this section the results of the 4km runs are compared to the observations.

5.3.1 IR Imagery

Figure 5.6 compares the 12 and 4km cloud top temperature fields to the IR imagery. There are a few hints that the 4km run looks better. The cloud field is generally less smooth (obviously) but also the dry slot which is too pronounced in the 12km run is less so at 4km. Similarly the rear portion of the cloud head is less overdeveloped in the 4km model. There is more sign of structures due to convection behind the system. It should be remembered that this diagnostic only includes the large scale cloud so the appearance of these features implies that the model is doing more explicit convection.

5.3.2 Dropsondes

Given that it was found (section 4.2.2) that the dropsonde cross sections have insufficient horizontal resolution for detailed comparison with the 12km model there is likely to be little benefit from using them to verify the 4km one. However it is still of interest to look at the RMS error statistics. These are shown in table 5.1.

	Temp RMS error (K)	**RH(ice) RMS error (%)**	**U,V magnitude RMS error (m/s)**
New Dynamics 12km	1.91	25.49	5.91
New Dynamics 4km	1.88	23.99	5.96

Table 5.1 RMS Errors for 12 and 4km New Dynamics runs compared to dropsondes

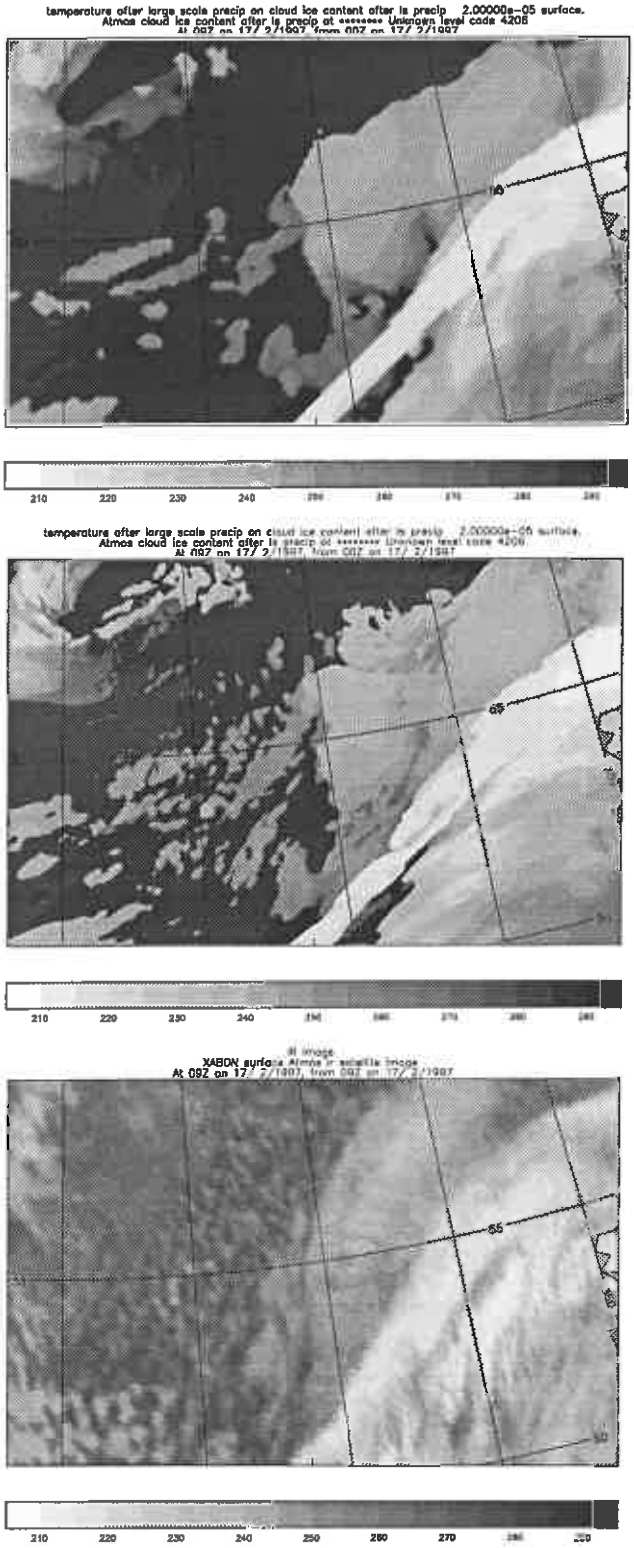

Figure 5.6 Cloud top temperature (2e-5 g/g threshold) from 12km (top) and 4km runs compared to IR image (bottom) for 9Z (i.e. T+9 forecast)

The RMS errors are very similar except for the RH (ice) where the error is a few per cent lower for the 4km run. However, as was discussed in section 4.2.2 the fact that similar RMS errors are seen in a higher resolution model with more variable fields would appear to be very encouraging

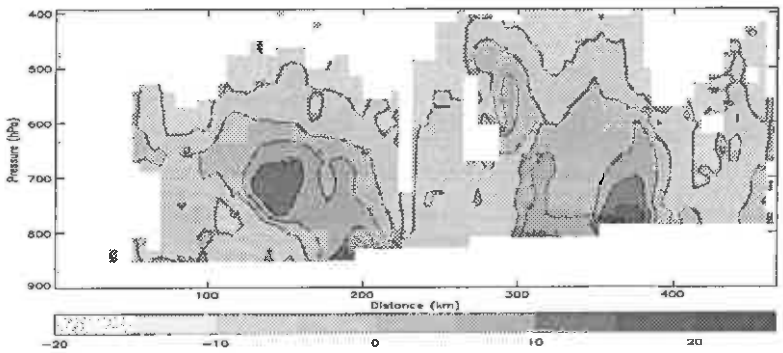

Figure 5.7 Radar reflectivity for run 1

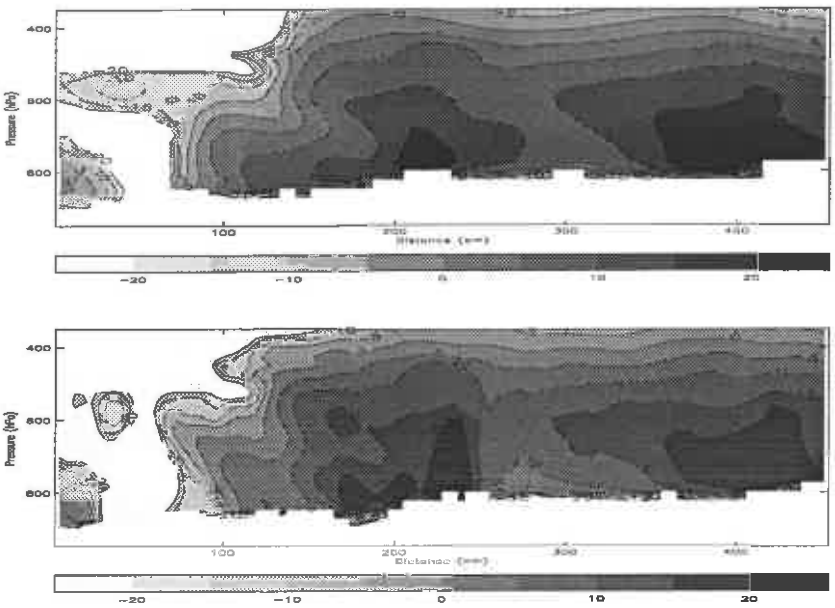

Figure 5.8 Simulated reflectivies for 12km (top) and 4km models (calculated above melting level only)

5.3.3 P-3 Radar

The conclusion of the comparison of the 12km runs to the P-3 radar was that the ice fields are too smooth in both models (section 4.2.3). It is therefore of interest to ask if this aspect appears significantly better at 4km resolution. This comparison is shown in

figures 5.7 (copy of figure 4.6 for convenience) and 5.8. The caveat that the reflectivity can only be calculated from the model above the melting level must again be remembered when looking at this however useful conclusions may still be drawn. The figure shows that there is no large change of the horizontal scale of variability of the ice fields between the two runs – the 12km model has slightly smoother fields but the difference is not great. It is also clear that there is little difference between the overall magnitudes of the reflectivity at the two resolutions – in both the reflectivies are substantially higher than in the observational data.

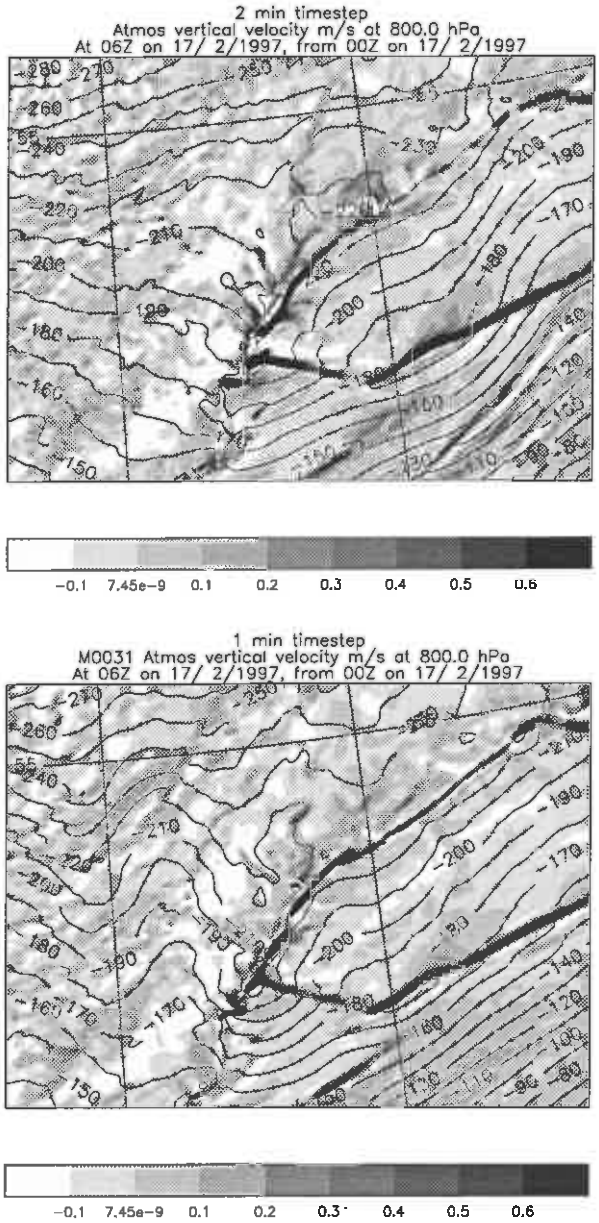

Figure 5.9 800hPa Vertical Velocity (shading) and 1000hPa geopotential height (contours) for 4km runs with 2 min (top) and 1 min timesteps at 6Z (T+6)

5.4 Other 4km Runs

So far only two variants on the 4km run described in the last section have been carried out. They are now briefly discussed.

5.4.1 Run with halved timestep

As mentioned in section 5.1 a worry with the 4km run is that the two minute timestep is rather long when it is considered that vertical velocities of up to 5 m/s are being produced. In order to address this a run was carried out with a halved timestep of 1 minute. The comparison of the 800hPa vertical velocity fields is shown in figure 5.9 shows there are significant differences between the runs The vertical velocity field shows that the fronts are generally more coherent, the overall values at the maxima are similar in both cases. The main difference in the vertical velocity fields is that the strips in the SE corner of the area of the figure are absent in the 1 minute run. In the light of the fact that changing the timestep does cause significant changes to the fields more work is required to determine the optimal value

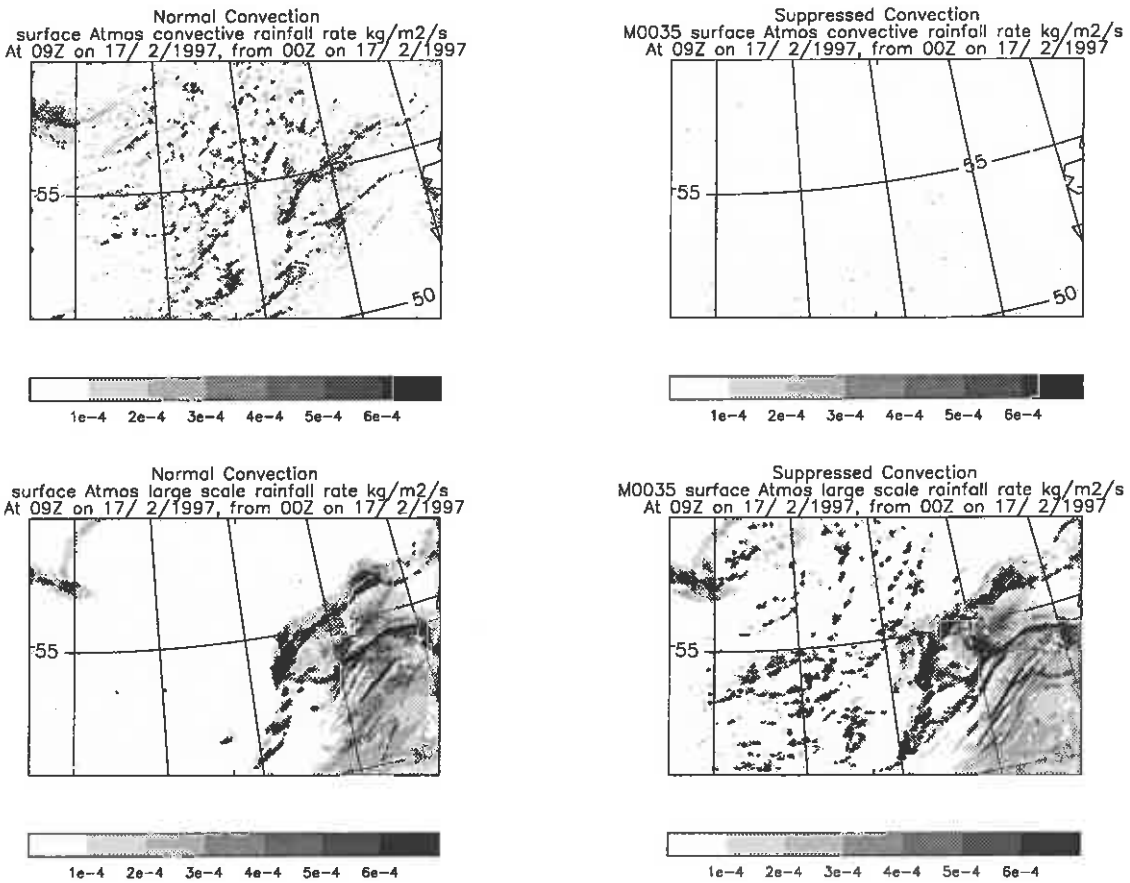

Figure 5.10 Convective and Large scale rain for models with normal and suppressed convection.

5.4.2 Run with Convection Suppressed

A subject which is likely to become important in the move towards high resolution operational models is the handling of convection. The current model at 4km is likely to be in an intermediate regime for this being too coarse to handle convection explicitly and yet possibly too high resolution for current convection schemes. It was mentioned earlier (fig 5.4) that the convective rain being produced by the model, in fact, looks quite realistic in its distribution. This section describes the first experiment towards probing the behaviour of convection in the model. This was simply to suppress the activity of the convection scheme and see if and how the model then handles the convection in an explicit sense. This was accomplished by simply setting the CAPE closure timescale to a very large value (10^6s) which would make any convective adjustment negligibly slow.

The results for the large scale and convective precipitation are shown in figure 5.10. The convective rain rate for the run with the convection suppressed can, indeed, be seen to be virtually zero which is confirmation that increasing the CAPE closure time is, indeed, having the effect intended. It is worth noting that the model appears to run happily without significant convective adjustment. The large scale rain rate for this run does have some convective cell like features in the region of convection to the W of the system. The area averaged rainrate over the system is encouragingly only a few per cent less than when the model is run with the convection scheme. The convective cells are, however, qualitatively different from those observed in the convective rain in the normal run in that they are less dense, larger and have higher rain rates. The cells are typically about 30km across and 60km apart compared to typically 8km across and separated by 15km in the normal run. The horizontal scale of the organisation appears to have got larger which is obviously likely to be related to the model gridlength. This test is, however, encouraging in that, even at these relatively coarse resolutions, the model makes a reasonably sensible attempt to reproduce explicit convection. Clearly more work is required to understand in more detail what is happening here and to understand what changes would be needed to the convection scheme to run an operational model at these resolutions.

6. 2km Simulations

In this section the 2km simulations of this case are briefly described. These results should be regarded as preliminary and will be discussed further in a future report.

6.1 Model details and Overview of Preliminary Results

The model has been run at 0.018 degree (approx. 2km) resolution on a 350x200 grid over a domain extending westwards from an eastern boundary about 200km west of the Irish coast (figure 6.1 shows data over the whole domain). When working at these resolutions on a rapidly moving system such as this it is clear that with any practical grid size the system will always pass through the model domain within a few hours. Hence, in contrast to the 4km case, no attempt was made to have a domain large enough to encompass the whole development – it was chosen so that the system would be roughly in the centre at 9Z. This model was also run at 45 level vertical resolution which is expected to be insufficient in this case but was the only thing

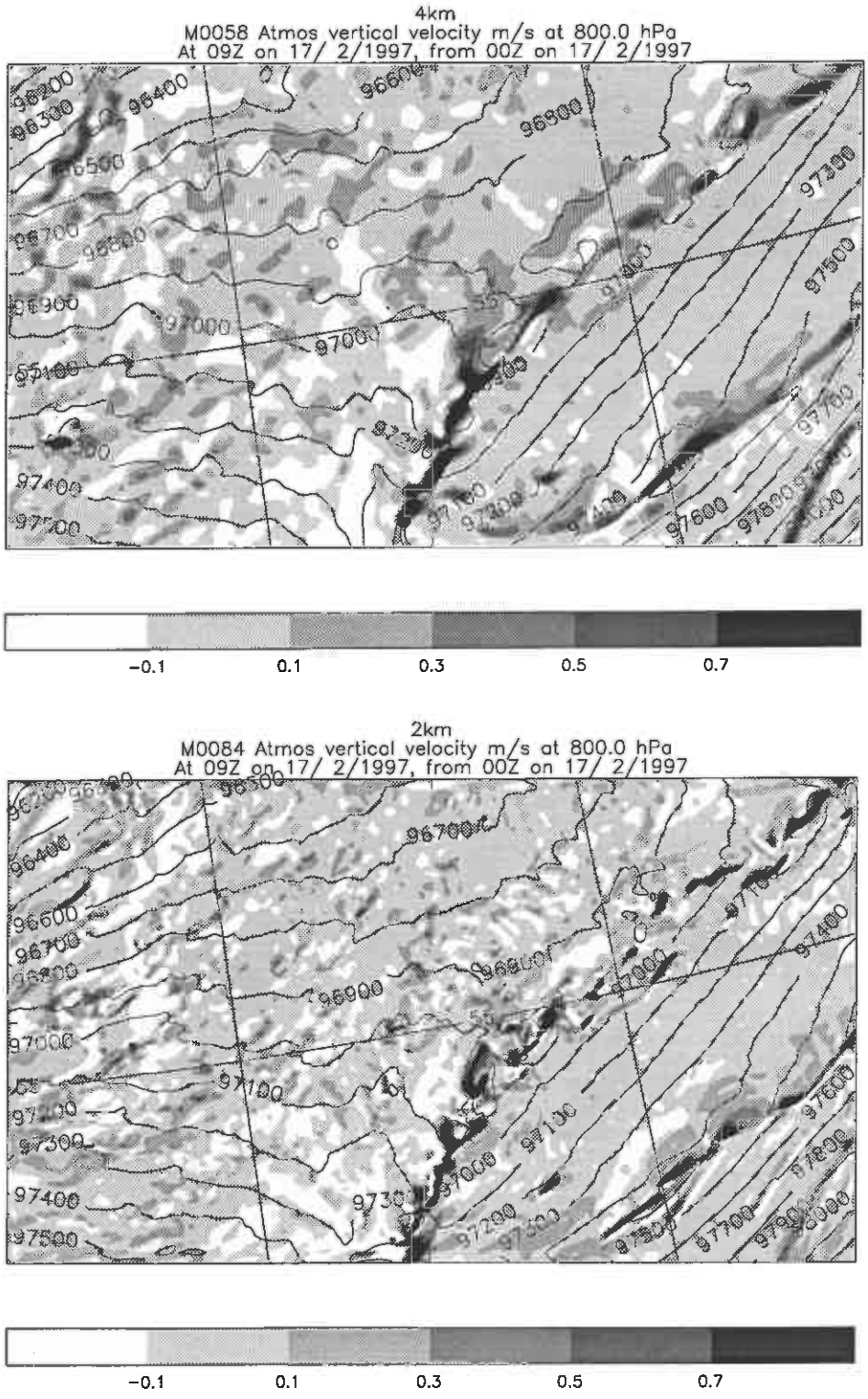

Figure 6.1 800hPa vertical velocity (shading) and pmsl (contours) for 4km model (top) and 2km.

currently possible without a lot of work. This is one reason why these results should be regarded as preliminary. Future work will assess the affect of vertical resolution. The model was again initialised with the 0Z 12km UM analysis and used boundary

data obtained from the 4km model. In order to save disc space with the more frequent boundary updating this model was only run forward to 10Z.

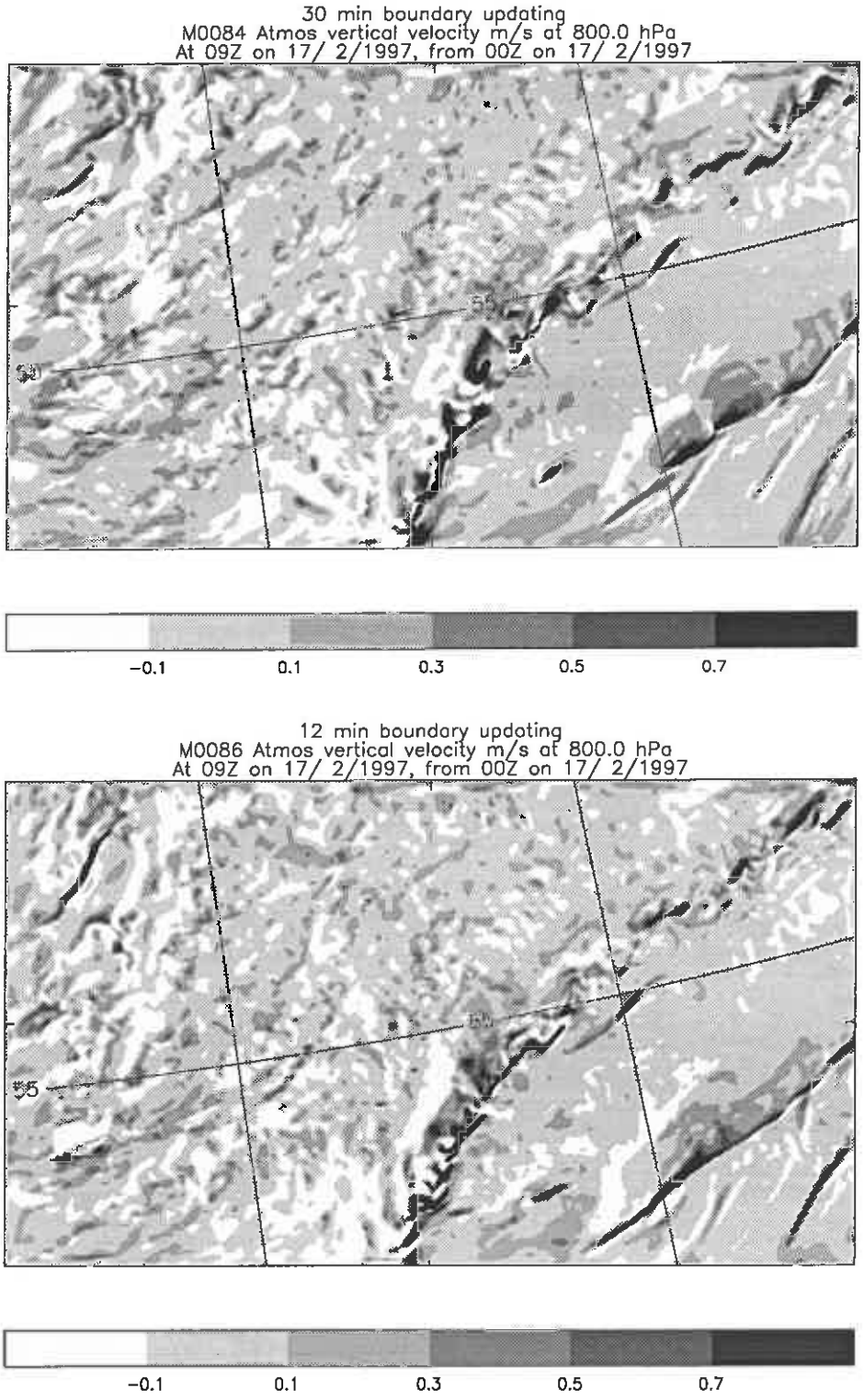

Figure 6.2 800hPa vertical velocity for 2km model at T+9 for run with 30 min boundary updating (top) and 12 minute updating.

The model was initially run with 60s timestep and 30 minute boundary updating. As previously no horizontal diffusion was used except on the top two levels. The results of this run are compared to the 4km model in figure 6.1

The broad results are very similar between the two models although as would be expected the fronts and other features are sharper in the 2km model. The maximum value of vertical velocity along the fronts is approximately $6ms^{-1}$ in the 4km model but $14ms^{-1}$ in the 2km model. As might be expected the fronts collapse down to close to 1 gridpoint in width in both models. The cross frontal circulations look very similar in cross section in the 2km model to those in the 4km model which is not surprising given the same vertical resolution.

Attempts were made at objective verification by calculating the RMS errors from the FASTEX dropsondes as for the 12 and 4km models. Unfortunately this analysis is hindered for the 2km model because the number of dropsondes available for the calculation is drastically reduced partly because some fall outside the domain and also because of the limited length of the run. The statistics are therefore of questionable validity and are not quoted here although the indications are that the 2km model is not significantly worse (or better) than the 4km one.

Two experiments have been carried out on the 2km model. Firstly the convection scheme was suppressed, as described in section 5.4.2 for the 4km model with very similar results. The main conclusion was again model runs satisfactorily without convection. There is little change in the vicinity of the system and again some scale change in the convective cells behind it. In the run with convection the cells are about the same size and spacing as in the 4km model (i.e. about 8km across and 30km apart). In the run with the convection scheme suppressed the cells are still about 8km across but are now separated by about 60km (the size is therefore reduced by about a factor of 3 from the 4km run without convection but the spacing is unchanged). The area averaged rain rate, however, is only a few per cent different between the runs with and without the convection scheme which is a similar difference to that seen in the case of the 4km model.

Secondly there were suspicions that some of the break up of fronts observed in the 2km model could be due to the boundaries being updated too infrequently (as discussed in section 5.2 in the case of the 4km model). In order to test this the model was rerun with 12 minute boundary updating. The results are compared to those with 30 minute updating in figure 6.2. It is clear that changing from 30 to 12 minute boundary updating makes a significant difference to the amount the front breaks up (particularly the front in the lower right hand corner which is not surprising since it is close to the boundaries) with less breaking up with more frequent updating. There is also the impression that the fronts are narrower with more frequent updating which would also be expected since they are less averaged over shorter distances between update times. This reinforces the conclusion reached with the 4km model that more work needs to be done on boundary data strategies with high resolution models.

7. Conclusions

- The New Dynamics model has been successfully run on the FASTEX IOP16 case multiply nested at 12, 4 and 2km resolution.

- Subjectively the 12km New Dynamics model appears to be at least as good as the UM at the same resolution. Many features are sharper and more coherent than in the UM which appears to be associated with the lack of horizontal diffusion.

- Only limited quantitative verification has been possible but at 12km the New Dynamics is slightly better against the FASTEX dropsondes than the UM and the 4km model is slightly better again. There is some indication that the 2km model is about the same as the 4km one.

- At 4 and 2km there are signs of explicit convection occurring in the cold air outbreak behind the system. The model runs satisfactorily without the convection scheme but the scales of the cells in the cold air outbreak are subjectively more realistic with it switched on.

This work has highlighted the following aspects which need further investigation:

1. The apparent instability of the model when adding levels of diffusion which should theoretically be stable.

2. Sensitivity to the number of vertical levels.

3. Lack of LS precipitation in cold air outbreak region in 2 and 4km runs (where a convective cell like structure is seen in the vertical velocity)

4. The high cloud liquid water content above the melting level in the New Dynamics model as compared to the UM.

5. The high cloud ice concentrations in both models compared to the radar data.

6. Quantitative verification.

Currently work is being carried out to make systematic comparisons of the performance of the New Dynamics on this case at 60,24,12,4,2km resolutions with particular emphasis on looking at the results of averaging the higher resolution data to the lower resolutions. This work will be reported on shortly.

Acknowledgements

The following have contributed significantly to this work:

P. Clark, N Roberts, R Forbes (JCMM)

Z Gardner, A Malcolm (New Dynamics group)

Clive Jones (ancillary generation)

CETP (radar data)

References.

A Staniforth et al. UMDP 15 (2000) "New Dynamics Formulation"

S Clough et al. (1998) JCMM Internal Report 81 "A JCMM Overview of FASTEX IOPs"

R Forbes et al (2000a) JCMM Internal Report 106 "The objective analysis of dropsonde data from FASTEX"

R Forbes, H Lean, N Roberts and P Clark (2000b) JCMM Internal Report 107 "Implications for Mesoscale Modelling from a Study of the FASTEX IOP16 Mid-latitude Cyclone"

A Macdonald (1999) Mon. Wea. Rev. **127**(9) 1985-1993 "An Examination of Alternative Extrapolations to Find the Departure Point Position in a Two-Time-Level Semi-Lagrangian Integration"

CURRENT JCMM INTERNAL REPORTS

This series of JCMM Internal Reports, initiated in 1993, contains unpublished reports and also versions of articles submitted for publication. The complete set of Internal Reports is available from the National Meteorological Library on loan, if required.

1. **Research strategy and programme**
   K A Browning et al
   January 1993

2. **The GEWEX Cloud System Study (GCSS)**
   GEWEX Cloud System Science Team
   January 1993

3. **Evolution of a mesoscale upper tropospheric vorticity maximum and comma cloud from a cloud-free two dimensional potential vorticity anomaly**
   K A Browning
   January 1993

4. **The global energy and water cycle**
   K A Browning
   July 1993

5. **Structure of a midlatitude cyclone before occlusion**
   K A Browning and N Roberts
   July 1993

6. **Developments in systems and tools for weather forecasting**
   K A Browning and G Szejwach
   July 1993

7. **Diagnostic study of a narrow cold frontal rainband and severe winds associated with a stratospheric intrusion**
   K A Browning and R Reynolds
   August 1993

8. **Survey of perceived priority issues in the parametrizations of cloud-related processes in GCMs**
   K A Browning
   September 1993

9. **The effect of rain on longwave radiation**
   I Dharssi
   September 1993

10. **Cloud microphysical processes - a description of the parametrization used in the large eddy model**
    H Swann
    October 1993

11. **An appreciation of the meteorological research of Ernst Kleinschmidt**
    A J Thorpe
    May 1992

12. **Potential vorticity of flow along the Alps**
    A J Thorpe, H Volkert and Dietrich Heimann
    August 1992

13. **The representation of fronts**
    A J Thorpe
    January 1993

14. **A parametrization scheme for symmetric instability: test for an idealised flow**
C S Chan and A J Thorpe
February 1993

15. **The Fronts 92 Experiment: a Quicklook Atlas**
Edited by T D Hewson
November 1993

16. **Frontal wave stability during moist deformation frontogenesis**
Part 1: Linear wave dynamics
C H Bishop and A J Thorpe
May 1993

17. **Frontal wave stability during moist deformation frontogenesis**
Part 2. The suppression of non-linear wave development
C H Bishop and A J Thorpe
May 1993

18. **Gravity waves in sheared ducts**
S Monserrat and A J Thorpe
October 1993

19. **Potential vorticity and the electrostatics analogy: quasi-geostrophic theory**
C Bishop and A J Thorpe
November 1993

20. **Recent advances in the measurement of precipitation by radar**
A J Illingworth
April 1993

21. **Micro-physique et givrage: cloud microphysics and aircraft icing**
A J Illingworth
May 1993

22. **Differential phase measurements of precipitation**
M Blackman and A J Illingworth
May 1993

23. **Estimation of effective radius of cloud particles from the radar reflectivity**
N I Fox and A J Illingworth
May 1993

24. **A simple method of Dopplerising a pulsed magnetron radar**
A Hua, A J Illingworth and J Eastment
November 1993

25. **Radiation and polar lows**
George C Craig
February 1994

26. **Collected preprints submitted to the International Symposium on the Life Cycles of Extratropical Cyclones; Bergen, Norway, 27 June - 1 July 1994**
April 1994

27. **Convective frontogenesis**
Douglas J Parker and Alan J Thorpe
April 1994

28. **Improved measurement of the ice water content in cirrus using a total water evaporator**
Philip R A Brown and Peter N Francis
April 1994

29. **Mesoscale effects of a dry intrusion within a vigorous cyclone**
K A Browning and B W Golding
April 1994

30. **GEWEX Cloud System Study, Science Plan**
May 1994

31. **Parametrization of momentum transport by convectively generated gravity waves**
R Kershaw
May 1994

32. **Mesoscale Modelling Newsletter No 5**
May 1994

33. **Observations of the mesoscale sub-structure in the cold air of a developing frontal cyclone**
K A Browning, S A Clough, C S A Davitt, N M Roberts and T D Hewson
May 1994

34. **Longwave radiative forcing of a simulated tropical squall line**
Imtiaz Dharssi
July 1994

35. **On the nature of the convective circulation at a kata-cold front**
K A Browning
September 1994

36. **Collective preprints of papers submitted to the COST-75 International Seminar on Advanced Weather Radar Systems, Brussels, 20-23 September 1994**
November 1994

37. **Use of satellite imagery to diagnose events leading to frontal thunderstorms: Parts I and II of a case study**
K A Browning and N M Roberts
November 1994

38. **The role of spaceborne millimetre-wave radar in the global monitoring of ice cloud**
P R A Brown, A J Illingworth, A J Heymsfield, G M McFarquhar, K A Browning and M Gosset
December 1994

39. **Potential vorticity inversion**
Michal Ziemianski
October 1994

40. **Theory of mature tropical cyclones; a comparison between Kleinschmidt (1951) and Emanuel (1986)**
Suzanne L Gray
December 1994

41. **Dispersion and removal of pollutants during the passage of an atmospheric frontal system**
N R Gimson
December 1994

42. **The role of snow sublimation in frontogenesis**
D J Parker and A J Thorpe
December 1994

43. **Potential vorticity and the electrostatics Analogy: Ertel-Rossby formulation**
A J Thorpe and C H Bishop
December 1994

44. **Mesoscale aspect of extratropical cyclones: an observational perspective**
K A Browning
January 1995

45. **A polar low outbreak: evolution and mesoscale structures**
T D Hewson, G C Craig and C Claud
February 1995

46. **Generation of near-surface gusts of deep convection**
K Nakamura and R Kershaw
April 1995

47. **Attribution concepts applied to the Omega Equation**
S A Clough, C S A Davitt and A J Thorpe
June 1995

48. **Parametrization of mixed-phase cloud and precipitation**
Susan P Ballard and M Gerard Hutchinson
June 1995

49. **Short-range forecasting of stratocumulus: initialization prediction**
Susan P Ballard, Simon D Jackson and B Macpherson
June 1995

50. **Contributions of the JCMM/Dept of Meteorology Radar Group to the 27th AMS Radar Meteorology Conference, Vail October 1995**
June 1995

51. **Cold pools in shear**
Douglas J Parker
September 1995

52. **High-resolution analysis of frontal fracture**
K A Browning, S P Ballard and C S A Davitt
September 1995

53. **The albedo of broken cloud fields: calculations using a modified two stream radiation code**
Imtiaz Dharssi and Roy Kershaw
October 1995

54. **Parametrization of momentum transport by convection. I: theory and cloud modelling results**
R Kershaw and D Gregory
November 1995

55. **Variation of frontal structure along a cold front**
K A Browning and N M Roberts
November 1995

56. **Secondary frontal waves**
Douglas Parker
December 1995

57. **Objective fronts**
T D Hewson
March 1996

58. **Mesoscale analysis of the activation of a cold front during cyclogenesis**
K A Browning, N M Roberts and A J Illingworth
June 1996

59. **Investigation of different representations of rain in a 1-d evaporation model**
H Swann
May 1996

60. **Parametrization of diabatic processes in the inversion of the omega-equation**
M Athanassiadou and A J Thorpe
June 1996

61. **The role of the environmental flow in the development of secondary frontal cyclones**
I A Renfrew, A J Thorpe and A Joly
June 1996

62. **Consequences of the geostrophic momentum approximation on barotropic instability**
S Malardel, A J Thorpe and A Joly
June 1996

63. **Contributions to the AMS/RMS Conference on Mesoscale Processes**
Reading, 9-13 September 1996

64. **Vorticity and potential vorticity in stratified flows interacting with an isolated obstacle**
Jorge A Gutiérrez and A J Thorpe
September 1996

65. **Triple point development: two case studies**
Douglas Parker
September 1996

66. **Radar observations of wind-shear splitting within evolving atmospheric Kelvin-Helmholtz billows**
D Chapman and K A Browning
April 1997

67. **Cold frontal structure derived from radar wind profilers**
K A Browning, D Jerrett, J Nash, T Oakley and N M Roberts
May 1997

68. **The dry intrusion and its effect on the frontal, cloud and precipitation structure of extratropical cyclones**
K A Browning - Text of invited special lecture at the Spring Conference
of the Meteorological Society of Japan, University of Tsukuba, 22 May 1997

69. **Met. Office Unified Model data, diagnostics, graphics programs, and other observational data available from the JCMM through the aegis of the Universities Weather Research Network (UWERN).** (Plus supplement)
Peter Panagi and Ed Dicks
June 1997

70. **Contributions of the JCMM/Dept of Meteorology Radar Group to the 28th AMS Radar Meteorology Conference.** Austin, Texas
September 1997

71. **Sensitivity of short-range weather forecasts to local potential vorticity modifications**
Meral Demirtas and Alan Thorpe
July 1997

72. **Objective identification of frontal wave cyclones**
T D Hewson
August 1997

73. **Attribution and its application to mesoscale structure associated with tropopause folds**
A J Thorpe
September 1997

74. **The role of the environmental flow in the development of secondary frontal cyclones**
Ian A Renfrew, Alan J Thorpe and Craig H Bishop
September 1997

75. **Potential vorticity: a short history of its definitions and uses**
Alan J Thorpe and Hans Volkert
September 1997

76. **Superposing semi-geostrophic potential vorticity anomalies**
H R Birkett and A J Thorpe
September 1997

77. **Short period forecasting of catchment-scale precipitation.**
Part 1: the role of Numerical Weather Prediction
M A Pedder, M Haile and A J Thorpe
September 1997

78. **Verification of the tracking technique used in an experimental cloud motion wind inferring system**
Z Wang, K A Browning and G A Kelly
October 1997

79. **A preliminary study of Fourier series analysis for cloud tracking with GOES high temporal resolution images**
Z Wang
October 1997

80. **Analysis of an ex-tropical cyclone after reintensifying as a warm-core extratropical cyclone**
K A Browning, G Vaughan and P Panagi
November 1997

81. **A JCMM overview of FASTEX IOPs**
S A Clough, H W Lean, N M Roberts, H Birkett, J-P Chaboureau, R Dixon, M Griffiths, T D Hewson and A Montani
January 1998

82. **Programs for PV inversion and modification**
Meral Demirtas
December 1997

83. **Release of potential shearing instability in warm frontal zones**
D Chapman and K A Browning
February 1998

84. **The European Cloud-Resolving Modelling Programme (EUCREM)**
Summary Report from the coordinator
P W White
April 1998

85. **A frontal wave database**
T D Hewson
April 1998

86. **Layering observed in dropsoundings from IOP 1 of Fronts 92**
S A Clough
May 1998

87. **Use of wind-shear displays for Doppler radar data**
D Chapman and K A Browning
May 1998

88. **Radar estimates of rainfall rates at the ground in bright band and non-bright band events**
T J Smyth and A J Illingworth
June 1998

89. **Correction for attenuation of radar reflectivity using polarisation data**
T J Smyth and A J Illingworth
June 1998

90. **The effects of convection on chemical reactions and precipitation scavenging**
Neil R Gimson
July 1998

91. **How to use the display program DISP**
Nigel Roberts
August 1998

92. **Conceptual models of cyclogenesis**
Adrian T Semple
August 1998

93. **Observations of oblate hail using dual polarisation radar and implications for hail detection schemes**
T J Smyth, T M Blackman and A J Illingworth
September 1998

94. **The semigeostrophic diagnosis of vertical motion. Part I: Formulation and co-ordinate transformations**
Mike A Pedder and Alan J Thorpe
September 1998

95. **The semigeostrophic diagnosis of vertical motion. Part II: Results for an idealised baroclinic wave life cycle**
Alan J Thorpe and Mike A Pedder
September 1998

96. **Convective destabilisation by a tropopause fold diagnosed using potential vorticity inversion**
Morwenna Griffiths, Alan Thorpe and Keith Browning
October 1998

97. **Forecast skill of the ECMWF model using targeted observations during FASTEX**
A Montani, A J Thorpe, R Buizza and P Unden
October 1998

98. **Observations and model simulations of the FASTEX IOP 16 frontal wave - effects of sublimation**
Sid A Clough, Humphrey W Lean, Nigel M Roberts and Richard M Forbes
December 1998

99. **The application of conceptual models in NWP**
Adrian T Semple
January 1999

100. **Mesoscale analysis of arc rainbands in a dry slot**
K A Browning and N M Roberts
January 1999

101. **Interaction of mesoscale tropopause depressions with a warm-core cyclone: observational and model analyses, and sensitivity to analysis errors**
K A Browning, A J Thorpe, A Montani, D Parsons, M Griffiths, P Panagi and E M Dicks
February 1999

102. **The use of water vapour imagery and PV inversion to adjust initial conditions in NWP**
Sean J Swarbrick
February 1999
This report is no longer available; see Internal Report No.108

103. **Summary notes for a lecture course on Waves in the Atmosphere and Ocean**
A A White
March 1999

104. **Results of a questionnaire on the operational value of conceptual models (CMs) of fronts and cyclones**
N M Roberts & M V Young
July 1999

105. **Contributions to the Poster Session at the 1998 UWERN Annual Science Meeting**
assembled by A A White
August 1999

106. **The objective analysis of dropsonde data from FASTEX**
Richard Forbes, Sid Clough, Mark Dixon, Andy Macallan & Nigel Roberts
January 2000

107. *NWP Technical Report No.302*
Implications for Mesoscale Modelling from a Study of the FASTEX IOP 16 Mid-latitude Cyclone
Richard M Forbes, Humphrey W Lean, Nigel M Roberts and Peter A Clark
March 2000

108. *NWP Technical Report No.291*
The use of water vapour imagery and PV inversion to adjust initial conditions in NWP
Final Project Report
Sean J Swarbrick
September 1999

109. *NWP Technical Report No.294*
A guide to aspects of water vapour imagery interpretation: the significance of dry regions
Nigel M Roberts
January 2000

110. *NWP Technical Report No.300*
The relationship between water vapour imagery and thunderstorms
Nigel M Roberts
February 2000

111. *NWP Technical Report No.293*
Holomorphic structures in hydrodynamical models of nearly geostrophic flow
V N Roubtsov and I Roulstone
January 2000

112. *NWP Technical Report No.301*
Multi-sensor synthesis of the mesoscale structure of a cold-air comma cloud system
K A Browning, P Panagi and E M Dicks
March 2000

113. *NWP Technical Report No.307*
Observations of stratospheric air entering the circulation of a polar low
K A Browning and E M Dicks
May 2000

114. *NWP Technical Report No.309*
Wind profiler – Unified Model comparison statistics
Peter Panagi & Ed Dicks
March 2000

115. *NWP Technical Report No.310*
Towards a similarity theory of moist convective updrafts
Olaf Stiller and George C Craig
May 2000

116. *NWP Technical Report No.312*
The mystery of striated cloud heads in satellite imagery
R S Dixon, K A Browning and G J Shutts
April 2000

117. *NWP Technical Report No.313*
MDIAG: a Fortran 90 program to compute diagnostics on pressure levels from Unified Model data on model levels
Peter Panagi
June 2000

118. *NWP Scientific Paper No.56*
Rearrangements of functions with applications to meteorology and ideal fluid flow
R J Douglas
June 2000

119. *NWP Technical Report No.320*
Tests of New Dynamics Model on the FASTEX IOP16 case
Humphrey Lean
September 2000

Met Office Joint Centre for Mesoscale Meteorology Department of Meteorology
University of Reading PO Box 243 Reading RG6 6BB United Kingdom
Tel: +44 (0)118 931 8425 Fax: +44 (0)118 931 8791
www.metoffice.com